Journal of Controlled Release 332 (2021) 636–651

Contents lists available at ScienceDirect

Journal of Controlled Release

journal homepage: www.elsevier.com/locate/jconrel

# Targeted delivery of mycophenolic acid to the mesenteric lymph node using a triglyceride mimetic prodrug approach enhances gut-specific immunomodulation in mice

Ruby Kochappan [a,b], Enyuan Cao [a,b], Sifei Han [a,b,*], Luojuan Hu [a,b], Tim Quach [b,c], Danielle Senyschyn [a,b], Vilena Ivanova Ferreira [a,b], Given Lee [a,b], Nathania Leong [a], Garima Sharma [a], Shea Fern Lim [b,c], Cameron J. Nowell [d], Ziqi Chen [e], Ulrich H. von Andrian [e], Daniel Bonner [f], Justine D. Mintern [g], Jamie S. Simpson [c,f], Natalie L. Trevaskis [a,*], Christopher J. H. Porter [a,b,*]

[a] Drug Delivery, Disposition and Dynamics, Monash Institute of Pharmaceutical Sciences, Monash University, Melbourne, Victoria 3052, Australia
[b] ARC Centre of Excellence in Convergent Bio-Nano Science and Technology, Monash Institute of Pharmaceutical Sciences, Monash University, Melbourne, Victoria 3052, Australia
[c] Medicinal Chemistry, Monash Institute of Pharmaceutical Sciences, Monash University, Melbourne, Victoria 3052, Australia
[d] Drug Discovery Biology, Monash Institute of Pharmaceutical Sciences, Monash University, Melbourne, Victoria 3052, Australia
[e] Dept. of Immunology, Harvard Medical School and Ragon Institute of MGH, MIT and Harvard, 77 Ave. Louis Pasteur, Boston, MA 02115, USA
[f] PureTech Health, 6 Tide Street, Boston, MA 02210, USA
[g] Department of Biochemistry and Molecular Biology, The University of Melbourne, Bio21 Molecular Science and Biotechnology Institute, Parkville, Victoria 3010, Australia

ARTICLE INFO

*Keywords:*
Lymph
Targeted drug delivery
Lipid
Prodrug
Immunomodulation
Mesenteric lymph node

ABSTRACT

The mesenteric lymph nodes (MLN) are a key site for the generation of adaptive immune responses to gut-derived antigenic material and immune cells within the MLN contribute to the pathophysiology of a range of conditions including inflammatory and autoimmune diseases, viral infections, graft versus host disease and cancer. Targeting immunomodulating drugs to the MLN may thus be beneficial in a range of conditions. This paper investigates the potential benefit of targeting a model immunosuppressant drug, mycophenolic acid (MPA), to T cells in the MLN, using a triglyceride (TG) mimetic prodrug approach. We confirmed that administration of MPA in the TG prodrug form (MPA-TG), increased lymphatic transport of MPA-related species 83-fold and increased MLN concentrations of MPA >20 fold, when compared to MPA alone, for up to 4 h in mice. At the same time, the plasma exposure of MPA and MPA-TG was similar, limiting the opportunity for systemic side effects. Confocal microscopy and flow cytometry studies with a fluorescent model prodrug (Bodipy-TG) revealed that the prodrug accumulated in the MLN cortex and paracortex at 5 and 10 h following administration and was highly associated with B cells and T cells that are found in these regions of the MLN. Finally, we demonstrated that MPA-TG was significantly more effective than MPA at inhibiting $CD4^+$ and $CD8^+$ T cell proliferation in the MLN of mice in response to an oral ovalbumin antigen challenge. In contrast, MPA-TG was no more effective than MPA at inhibiting T cell proliferation in peripheral LN when mice were challenged via SC administration of ovalbumin. This paper provides the first evidence of an *in vivo* pharmacodynamic benefit of targeting the MLN using a TG mimetic prodrug approach. The TG mimetic prodrug technology has the potential to benefit the treatment of a range of conditions where aberrant immune responses are initiated in gut-associated lymphoid tissues.

*Abbreviations:* APC, Antigen presenting cell; BDP-TG, Bodipy triglyceride prodrug; CM, chylomicron; CTV, CellTrace™ Violet; GIT, gastrointestinal tract; GALT, gut associated lymphoid tissue; HEV, high endothelial venule; HIV, human immunodeficiency virus; LBF, lipid-based formulation; LP, lipoproteins; LN, lymph node; MM, medullary macrophage; MLN, mesenteric lymph nodes; MPA, mycophenolic acid; MPA-TG, mycophenolic acid triglyceride prodrug; PK, pharmacokinetics; PLN, peripheral lymph nodes; SCS, subcapsular sinus; SCM, subcapsular sinus macrophage; SC, subcutaneous; TG, triglyceride; IV, intravenous; OVA, ovalbumin.

* Corresponding authors at: Drug Delivery, Disposition and Dynamics, Monash Institute of Pharmaceutical Sciences, Monash University, Melbourne, Australia.
*E-mail addresses:* sifei.han@monash.edu (S. Han), natalie.trevaskis@monash.edu (N.L. Trevaskis), chris.porter@monash.edu (C.J.H. Porter).

https://doi.org/10.1016/j.jconrel.2021.02.008
Received 21 September 2020; Received in revised form 7 February 2021; Accepted 8 February 2021
Available online 17 February 2021

## 1. Introduction

The lymphatic system comprises a network of lymphatic vessels, lymph nodes (LNs) and lymphoid tissues that play important roles in dietary lipid absorption, the maintenance of tissue fluid homeostasis and immune surveillance [1,2]. The lymphatics are also involved in the pathophysiology of conditions including lymphedema, cancer, obesity and metabolic diseases, graft versus host disease, and inflammatory and autoimmune diseases [3–7].

LNs are the main site of antigen presentation to lymphocytes by antigen presenting cells (APCs), leading to the generation of adaptive immunity [8–11]. Lymph enters the LN via afferent lymphatic vessels and exits via the efferent lymphatic vessel. Cells also populate the LN via specialised blood microvessels (high endothelial venules, HEV) [9,12]. Lymph that enters via afferent lymphatic vessels may pass around the circumference of the lymph node via a subcapsular sinus, be filtered by macrophages that line the subcapsular sinus (subcapsular sinus macrophages, SCM) or enter into the LN parenchyma via narrow conduits. The LN parenchyma is divided into three areas from the afferent (incoming) to efferent (outgoing) side: the cortex, paracortex and medulla. The cortex consists primarily of B-cell-rich follicle regions, while in the paracortex the major immune cells are T cells and APCs. The medulla, lined by medullary macrophages (MMs), is the primary site for maturation of antibody producing plasma cells and also contains T and B cells.

LNs are thus a harbour for immune cells and targeted delivery to the LN has the potential to enhance the efficacy of immunomodulating drugs in diseases such as organ transplantation [13,14], autoimmune diseases [15,16] and cancer [17,18]. LNs have also been identified as a major reservoir for infections including including human immunodeficiency virus (HIV) such that the efficacy of antiretroviral drugs is enhanced where increased accumulation in LNs occurs [19]. Finally, vaccines have been reported to be more effective when adjuvants and antigens are more directly delivered to LNs [20,21].

The role of LNs in immune surveillance is particularly notable in the gastrointestinal tract (GIT). The GIT is highly exposed to exogenous antigens from food, the environment and the large numbers of commensal bacteria ($\sim 10^{14}$ bacteria) in the large bowel [22]. To maintain the delicate balance between tolerance to food and self-antigens, and protection against the systemic entry of commensal and foreign bacteria, the GIT is protected by a network of gut associated lymphoid tissue (GALT) including the Peyer's patches, isolated lymphoid follicles and the mesenteric lymph nodes (MLN). Notably, the GALT harbours approximately 50–70% of the entire body lymphocyte pool and the MLN is considered to be the largest lymph node in the body in terms of size and cell number [23,24]. The immune response within MLN is also central to the development of oral tolerance [25] and the directed development of oral tolerance to various auto-antigens has led to improvements in a range of preclinical autoimmune models [26–29] (although clinical data remains equivocal). MLN are therefore a potentially important target site for the delivery of immunomodulatory agents to treat autoimmune diseases, food allergies, localised infection and cancer, and to improve the utility of vaccines. More broadly, the potential exists to manipulate immune events distal to the GIT environment, by targeting lymphocytes within the MLN that subsequently migrate to secondary lymphoid tissues in alternate locations via lymphocyte homing and recirculation pathways [30].

Directed delivery to the mesenteric lymphatic vessels and MLN can be achieved via integration into dietary lipid absorption pathways that drain into the mesenteric lymph. In this way, highly lipophilic drugs can associate with lipid absorption pathways following oral delivery and subsequently be transported via the mesenteric lymphatic vessels to the MLN [7]. Most currently used oral immunosuppressants, however, are small molecule drugs that are not sufficiently lipophilic to associate with lipid absorption pathways and are therefore not lymphatically transported after oral administration [7,31,32]. Instead, they are absorbed into the mesenteric blood capillaries and portal vein, and in doing so bypass the MLN during absorption [7]. In recent studies, we targeted the delivery of less lipophilic drugs, including the immunosuppressant mycophenolic acid (MPA), to the mesenteric lymphatics and MLN using lipid mimetic prodrug strategies that facilitate drug integration into intestinal lipid transport pathways [34,35]. The most successful strategy was a triglyceride (TG) mimetic approach where the drug (eg. MPA) was linked at the 2 position of a diglyceride (e.g. 1,3-dipalmitoyl-2-mycophenoloyl glycerol (MPA-TG) and this is described in Fig. 1.[37–40].

These previous studies [35] indicate the potential to provide enhanced *in vivo* immunomodulation, but to this point this has not be proven. Since MPA acts via inhibition of inosine monophosphate dehydrogenase (IMPDH), which is required for DNA replication in lymphocytes, lymphocyte targeting strategies for MPA might be expected to be beneficial. Here we therefore explored the potential pharmacodynamic benefits of targeting MPA to the MLN using the TG-prodrug strategy. First, we sought to provide evidence that the prodrug strategy enhances drug exposure to the MLN in mice. Second, we used detailed FACS and fluorescent microscopy analysis to profile the distribution of a fluorescent prodrug analogue to immune cells in the mouse MLN. The prodrug resulted in markedly higher exposure in the lymph, LN and immune cells. Finally, we aimed to provide *in vivo* proof of concept of enhanced GIT immunomodulation. To do this we employed a mouse oral ovalbumin (OVA) antigen challenge model. We show that treatment with MPA-TG is significantly more effective in inhibiting $CD4^+$ and $CD8^+$ T cell responses in the MLN after oral OVA challenge compared to MPA, providing support for the concept of MLN targeted, GIT specific, immunomodulation.

## 2. Materials and methods

### 2.1. Materials

The MPA prodrug MPA-TG was synthesised in house from MPA (>98%, AK Scientific, Palo Alto, CA, USA) as described previously [34]. A TG prodrug of bodipy carboxylic acid was similarly synthesised as shown in the Supplementary information. The structures of MPA, bodipy and the equivalent prodrugs are shown in Fig. 2.

Ketoprofen (internal standard), oleic acid, Tween 80, Triton™ X-100, phosphate buffered saline (PBS, pH 7.4) and sucrose were purchased from Sigma-Aldrich, MO, USA. Acetonitrile for liquid chromatography (LCMS grade) was purchased from Merck Pty Ltd., VIC, Australia. Ultrapure water was obtained from a Milli-Q™ system (Millipore, MA, USA). Bodipy-TG was synthesised in house (details in supplementary information) using the commercially available Bodipy intermediate, BDP 558/568 carboxylic acid (Lumiprobe, MD, USA). Menzel Glaser Superfrost Plus glass slides (ground edges) and ProLong™ Gold Antifade Mountant were obtained from Thermo Fischer Scientific, VIC, Australia. Paraformaldehyde, Tissue-Tek® optimal cutting temperature (OCT) compound manufactured by Sakura Finetek was supplied by Proscitech, QLD, Australia. Cryomoulds were purchased from TRAJAN, VIC, Australia. Ovalbumin (Grade V), propidium iodide solution, RPMI-1640 Medium with L-glutamine, sodium bicarbonate and bovine serum albumin (heat shock fraction, pH 7, ≥98%) were obtained from Sigma-Aldrich, MO, USA. CellTrace™ Violet Cell Proliferation Kit, absolute counting beads, phosphate buffered saline, fetal bovine serum were all obtained from Life Technologies, ThermoFisher Scientific, CA, USA. Flow cytometry antibodies: PE anti-mouse CD4, APC anti-mouse CD8a, FITC anti-mouse CD45.1 and FITC anti-mouse TCR Vα2 were obtained from Biolegend, CA. USA and sourced locally from Australian Bioresearch. For magnetic cell separation the $CD4^+$ T cell isolation kit for mouse, $CD8a^+$ T cell isolation kit for mouse, LS Column Adapter, VarioMACS Separator and LS Columns were from MACS, Miltenyi Biotec, NSW, Australia. All other chemicals were analytical grade or better.

### 2.2. Animals

Male and female C57BL/6 mice were obtained from the Monash Animal Research Platform, Victoria, Australia. All experiments were approved by the local animal ethics committee and were conducted in accordance with the *Australian and New Zealand Council for the Care of Animals in Research and Teaching Guidelines*. Mice were maintained on a standard diet with free access to water prior to experiments. Female OT-I and OT-II mice were obtained from either the Melbourne Bioresources Platform at Bio21 Molecular Science and Biotechnology Institute or the Walter and Eliza Hall Institute (WEHI), Victoria, Australia. The Bio21 OT mice were OT-I × B6.SJL-Ptprc$^{a}$Pep3$^{b}$/BoyJ (OT-I x Ly5.1) and hence expressed CD45.1 (Ly5.1) antigen on lymphocytes to assist in differentiation by flow cytometry from the lymphocytes of recipient C57BL/6 mice which express the CD45.2 antigen [36]. The OT mice obtained from WEHI did not express the CD45.1 antigen and therefore a TCR Vα2 antibody was used alongside the presence of Celltrace$^{TM}$ Violet (CTV) staining to identify the adoptively transferred OT cells (mice were from the C57BL/6 background and expressed the CD45.2 antigen) [37]. Mice were maintained on a standard diet with free access to water prior to experiments. Female mice were employed for immune challenge studies as it has been reported that male hormones such as dihydrotestosterone (DHT) and testosterone have an immune suppressive effect [38,39] and this might lead to an abrogated immune response in the ovalbumin model. To allow direct correlation, female mice were therefore also used in pharmacokinetic and LN deposition studies. A combination of male and female animals were used in the lymph transport experiments.

### 2.3. Preparation of drug formulations

The compositions of the MPA and MPA-TG drug formulations for in vivo lymphatic transport, plasma pharmacokinetics (PK), lymph node exposure and immune challenge studies are given in Table 1. For the lymphatic transport studies, parent drug (MPA) was given as an aqueous solution and lipid-based formulation (LBF), while the prodrug (MPA-TG) was given as a LBF only since lipids are required to solubilise the drug and drive lymphatic transport.

The prodrug MPA-TG was prepared in a LBF containing 250–300 mg/kg oleic acid and 0.5% *w/v* Tween 80, as previously described (12, 14). Briefly, MPA-TG, Tween 80 and oleic acid were mixed in a glass vial as a lipid phase, heated at 60 °C for a minute and incubated at 37 °C for 6–8 h to equilibrate and to allow the prodrug to dissolve. The aqueous phase, consisting of PBS (pH 7.4) was subsequently added to the glass vial and the formulation was emulsified by ultrasonication with a Misonix XL 2020 ultrasonic processor (Misonix, Farmingdale, NY, USA) using a 3.2-mm microprobe tip at an amplitude of 240 μm and a frequency of 20 kHz for 2 min at room temperature.

For plasma pharmacokinetic, lymph node exposure and immune challenge studies, parent drug (MPA) was administered as a suspension in 0.5% *w/v* sodium carboxymethyl cellulose (CMC) in PBS, pH 7.4. For the MPA lymphatic transport studies, MPA was administered as an infusion over 1 h and, to avoid any settling of the suspension during the process, a solution (rather than a suspension) formulation was employed. For the MPA solution, a low dose of MPA was used due to its low aqueous solubility. The aqueous solution of MPA was obtained by dissolving MPA in PBS at a concentration of 0.5 mg/ml. 0.5 mL (i.e. 0.25 mg of MPA) was subsequently infused intraduodenally to anaesthetised mice. For the lipid-based MPA formulation, aqueous MPA in PBS solution (0.5 mg/ml) was added to a mixture of Tween and oleic acid similar in composition to the MPA-TG formulation, as described in Table 1 and sonicated as described previously for the prodrug [34].

Lymphatic transport studies were conducted at a relatively low dose (0.25 mg and 1 mg per mouse for MPA and MPA-TG, respectively), to facilitate the slow intraduodenal infusion of a solution formulation. For the plasma pharmacokinetic (PK), lymph node (LN) exposure and immune challenge studies, mice were administered higher doses: 1 mg of MPA and 2.77 mg prodrug (an equimolar quantity of MPA) since this dose was used to facilitate immunosuppression in the OVA challenge studies. For the imaging studies, a Bodipy-TG or parent Bodipy formulation was prepared in a similar way to the lipid formulation of MPA-TG, but replacing MPA-TG with Bodipy-TG or parent Bodipy. The volume of drug formulation administered via intraduodenal infusion was 0.5 mL. For experiments involving administration by oral gavage the volume administered was limited to 0.2 mL.

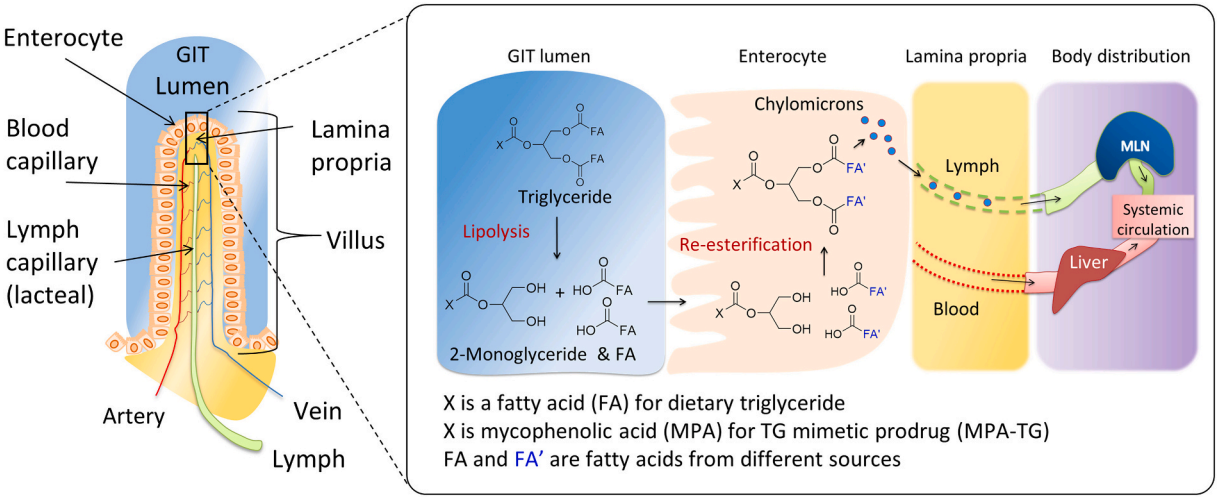


**Fig. 1.** The absorption and transport of dietary TG and the TG mimetic prodrug into the mesenteric lymphatics. Left: The intestinal villus is lined by enterocytes that make up the intestinal epithelium. Under the epithelial layer, in the lamina propria, blood and lymphatic vessels are present and are able to transport materials that are absorbed across the enterocytes back to the systemic circulation. Right: In the GIT lumen, TG (or the equivalent TG prodrug) is digested by lipases to release the 2-monoglyceride (2-MG) (or equivalent prodrug species) and fatty acids (FAs). The 2-MG and FAs are absorbed into enterocytes, where re-esterification of the 2-MG takes place to form new TG derivatives. These TG derivatives are then assembled into lipoproteins, primarily chylomicrons (CM), that are exocytosed into the underlying lamina propria. From here the CM (and any associated lipophilic drugs or prodrugs) preferentially gain access to the mesenteric lymphatics due to their relatively large size (100–1000 nm) providing direct access at high concentration to the MLN before draining into the systemic circulation.

### 2.4. Mesenteric lymph transport of MPA and MPA-TG

Male or female C57BL/6 mice were fasted for 2 h prior to surgery to reduce the potential for food effects on drug absorption. During the surgery, mice were anaesthetised using isoflurane (2–5% *v*/v in carbogen) and placed on a heated pad at 37 °C to maintain body temperature throughout anaesthesia. The mesenteric lymph duct cannulation was performed in mice as previously described in detail [40]. Briefly, abdominal skin from the midline ~0.5 cm below the ribs and above the right kidney was shaved, and a ~ 1 cm horizontal incision was made. The intestine was moved to the left side to locate the right kidney and the mesenteric lymph duct lying almost perpendicular to the kidney. The mesenteric lymph duct was identified and cleared of overlying membranes by blunt dissection. The duct was cannulated using a 0.2 mm i.d. and 0.5 mm o.d. polyethylene cannula (Microtube Extrusions, NSW, Australia) connected to a larger polyethylene cannula with 0.5 mm i.d. and 0.8 mm o.d. The cannula was sealed in place with a drop of Uhu® superglue (GmbH & Co. KG, Germany) after ensuring insertion into the mesenteric lymph duct. The duodenum was then cannulated using a 0.5 mm i.d. and 0.8 mm o.d. polyethylene cannula with a J-shaped hook to assist in securing it into the duodenum, as described previously [40]. The duodenal cannula was required to allow infusion of saline during rehydration and formulation during dosing. The mice were rehydrated for 0.5 h after surgery with saline at a rate of 0.3 ml/h controlled using an infusion pump (Model '11' Plus Syringe Pump, Harvard Apparatus, Holliston, MA, USA). After the rehydration period the (pro)drug formulation was administered at a rate of 0.5 ml/h for 1 h and lymph was collected every 1 to 2 h for 6 h into heparinised (5 μl of 10 IU hep saline) Eppendorf tubes. The mice were euthanized at the end of the experiment by intracardiac injection of 0.1 mLLethabarb® (Provet, VIC, Australia). The collected lymph was aliquoted and stored at −20 °C prior to analysis.

### 2.5. Plasma pharmacokinetics and LN exposure studies

The pharmacokinetics (PK) and LN exposure study was performed in female C57BL/6 mice using a population sampling approach and serial blood sampling (taking 2 samples from each mouse). In each mouse, one sample was taken from the submandibular vein and a final sample was taken by cardiac puncture prior to euthanasia. Data were collected from multiple animals to provide $n = 3$–4 mice at each time point.

For the single-dose PK study, the formulation was administered to non-fasted mice by oral gavage and 2 × 200 μL blood samples were taken from each mouse. Mice were randomised to provide $n = 3$–4 samples at times of predose (0 h) and 0.25, 0.5, 1, 2, 4 and 6 h post dose. Blood was collected into heparinised tubes using heparinised capillary tubes. Plasma was separated by centrifugation and plasma samples were aliquoted and stored at −20 °C until analysis. LN were collected after the terminal blood collection at 0.25, 1, 4 and 6 h. The mesenteric (upper and lower chain) and peripheral (inguinal, axillary, brachial and cervical) LN were collected into tubes and stored at −20 °C until analysis. The plasma and lymph node samples were analysed for MPA as described in supplementary section 7.

For the multiple-dose PK study, mice were gavaged with five consecutive doses, each separated by an interval of 10–12 h, under non-fasting conditions (mirroring the conditions in the OVA challenge study). Blood samples were collected on the morning of the third day after administration of the final dose. Blood samples were collected in a similar manner to that described for the single-dose PK study (2 samples from each mouse), with the sampling time points altered to 0.25, 0.5, 1, 2, 3 and 6 h. The collection timepoints for LN (including both mesenteric and peripheral as described above) were also slightly altered to 0.25, 0.5, 2 and 6 h to include an earlier time point after multiple dosing.

### 2.6. LN distribution of bodipy-TG (BDP-TG) by immunofluorescence microscopy

Female C57BL/6 mice were orally gavaged with 0.3 mg of BDP or BDP-TG (a fluorescent model prodrug) in a LBF as detailed in Table 1 in order to visualise the potential distribution of the prodrug in the MLN. Mice were sacrificed at 1, 5 or 10 h post-dose, and their MLN or peripheral lymph nodes (PLN) were obtained.

The LN collected were fixed in 4% paraformaldehyde in PBS solution for 12 h at 4 °C, washed with PBS and LN were embedded in 2% agarose gel. Lymph nodes were sectioned using a Vibratome (Leica, VT1000S, Wetzlar, Germany) at typically ~60 Hz frequency, ~0.05 mm/s blade

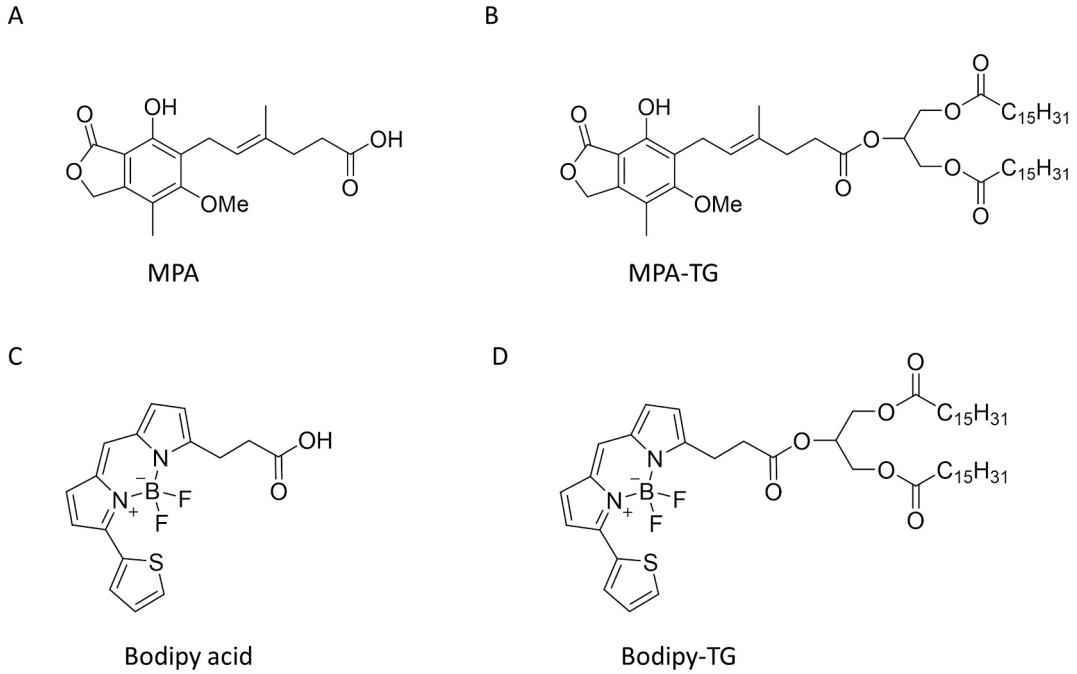


**Fig. 2.** Chemical structure of A) Mycophenolic acid (MPA), B) 1,3-dipalmitoyl-2-mycophenoloyl glycerol (MPA-TG), C) Bodipy acid and D) An analogue of 1,3-dipalmitoyl-2-(mycophenoloyl)glycerol where the 2-position is acylated with BDP 558 carboxylic acid (Bodipy-TG).

**Table 1**
Experimental study details including gender, formulation details, method of drug administration and animal conscious state.

| Study | Lymph transport | | | Plasma PK, LN exposure and immune challenge studies | | Imaging study | |
|---|---|---|---|---|---|---|---|
| Gender | Male/female | | | Female | | Female | |
| Conscious state | Anaesthetised | | | Conscious | | Conscious | |
| Method of administration | Intraduodenal infusion over 1 h | | | Oral gavage | | Oral gavage | |
| Volume dosed (mL) | 0.5 | | | 0.2 | | 0.2 | |
| Drug/Prodrug formulation | MPA (aqueous) | MPA (LBF) | MPA-TG (LBF) | MPA (suspension) | MPA-TG (LBF) | Bodipy-TG (LBF) | Bodipy parent (LBF) |
| Dose of drug/prodrug (mg) | 0.25 | 0.25 | 1 | 1 | 2.77 | 0.1-0.3 | 0.04 |
| Oleic acid (mg) | - | 7.5 | | - | 5.9 | 5.9 | |
| Tween 80 (mg) | - | 2.83 | | - | 1 | 1 | |
| Vehicle | PBS pH 7.4 | | | 0.5 % NaCMC in PBS pH 7.4 | PBS pH 7.4 | PBS pH 7.4 | |

PK - pharmacokinetics, LN - lymph nodes, LBF - lipid based formulation, NaCMC - sodium carboxymethylcellulose, PBS - phosphate buffered saline, MPA - mycophenolic acid, TG - triglyceride.

speed with ~1 mm amplitude, and up to 250 μm thickness to maintain the structural integrity of the nodes and to visualise spatial distribution of BDP and BDP-TG. Sections were blocked at room temperature using blocking buffer (3% BSA in PBST) for up to 2 h and then stained with the following primary antibodies (at 0.5 mg/ml, 1 in 200 dilution): rat-anti CD4 (Bio-Legend, CA, USA), rat anti-B220 conjugated with FITC (Bio-legend, CA, USA) for up to 1 day at room temperature with constant shaking. Sections were washed 3 times for 15 min each time and then incubated overnight with secondary antibodies (2 mg/ml, 1 in 500 dilution) against the host species of the primary antibody: goat anti-rat Alexa Fluoro 647 antibody (Life Technologies, CA, USA) in blocking buffer (% goat serum in PBS). Tissues were mounted using ProLong™ Gold Antifade Mountant (Thermo Fischer Scientific, VIC, AU).

The tissues were imaged using a Leica SP8 inverted confocal microscope with a 20× or 40× Plan Apo CS2 NA0.75 objective controlled by LAS AF (version 3.5.5) image acquisition and processing software (Leica, Wetzlar, Germany). Excitation/emission wavelengths were as follows: 495/550 nm for Alexa 488 (excited by 488 laser), 550/600 nm for Alexa 568 (excited by 568 laser) and 600/700 nm for Alexa 647 (excited by 633 laser). The image format was 512 × 512 or 1024 × 1024 pixels and scan frequency was 400–600 Hz. *Z*-stacks were obtained at a step size of 1–3 μm and images were captured as a tilescan and merged.

### 2.7. Flow cytometry analysis of immune cell association with BDP-TG in mesenteric LN

Female C57BL/6 mice were orally gavaged with 0.3 mg of BDP-TG in a LBF as detailed in Table 1. Upper and lower MLN were collected, pooled and punctured multiple times with a 21G needle to help digestion of the tissue. Lymph nodes were then digested in 500 μL of DMEM containing collagenase IV (1 mg/mL) and DNAse I (2 mg/ml, both from Roche, Basel, Switzerland). After digestion, lymph node cell suspensions were filtered through a 70 mm nylon cell strainer and resuspended in 1 mL 2% FBS in PBS. LN cell suspensions were stained with antibodies toward CD11c, CD11b, MHCII, CD19, F4/80, CD8a, CD45, CD3 and CD4 at the concentrations listed in supplementary Table S-1 in the dark at 4 °C for 15–20 min. After staining with antibodies, cells were fixed using Cytofix buffer (BD Biosciences, San Jose, CA, USA) for 10 min. Cells were then analysed using a Stratedigm S1000EON Benchtop Flow Cytometer (Stratedigm, Franklin Lakes, NJ, USA) and FlowJo software version 10 (Tree Star Inc., Ashland, OR, USA). All appropriate controls, including negative controls, compensation controls and fluorescence minus one (FMO) controls, were applied.

### 2.8. Purification and labelling of OVA specific T cells

OVA specific $CD4^+$ and $CD8^+$ T cells were purified from the LN of OT-II and OT-I mice, respectively, and were employed in independent experiments. LNs collected from OT mice (including MLN, inguinal, brachial, axillary, cervical and iliac LNs) were gently pushed through a 40 μm sieve using the back of a 1 mL syringe plunger, to form a single cell suspension in RPMI 1640 with 2% fetal bovine serum (FBS). T cells were then purified using a negative selection separation strategy that employed a magnet assisted cell sorting (MACS®) protocol from Miltenyi Biotec. The protocol provided in the kit supplied by Miltenyi Biotec was followed. Briefly cell suspensions obtained from the LNs of the OT mice were resuspended in MACS buffer (PBS with 2 mM EDTA and 0.2% *w/v* BSA) and labelled with antibodies against all other surface markers, except for the marker for the cells of interest. For $CD4^+$ T cells, cells were isolated by depletion of non $CD4^+$ T cells using a cocktail of biotin-conjugated antibodies against CD8a, CD11b, CD11c, CD19, CD45R (B220), CD49b (DX5), CD105, MHC-class II, Ter-119 and TCR γ/δ as the primary labelling reagent. For isolation of $CD8^+$ T cells, a similar cocktail of antibodies against non CD8+ T cells were used. The cells were then incubated with anti-biotin labelled magnetic microbeads and passed through a LS column in MACS buffer within the magnetic field of the Vario MACS separator. The labelled (unwanted) cells were retained within the column while the unlabelled cells flowed through the column and were collected. The quantity of all reagents employed was as per the description in the kit. The purity of the isolated cells was confirmed by flow cytometry of a small sample that was stained with antibodies specific for $CD4^+$ (OT-II) or $CD8^+$ (OT-I) T cells and for Ly5.1 where OT mice were intercrossed with Ly5.1 congenic mice or TCR Vα2. The purified $CD4^+$ or $CD8^+$ T cells were washed and resuspended in PBS containing 0.1% bovine serum albumin (BSA) and subsequently labelled with CTV dye to allow downstream quantification of cell replication. CTV labelling was performed in two steps [41,42]. First, the CTV dye was diluted 100 fold (from 5 mM to 50 μM) with 0.1% BSA in PBS. This solution was further diluted 10 fold (to 5 μM) by the process of addition to the cell suspension ($\leq 50 \times 10^6$ cells/ml) in a 10 mL Falcon tube. The tube was sealed and vortexed to allow even distribution of the dye to the cells. The number of purified and labelled OT cells was counted using a haemocytometer. The cells were then pelleted and resuspended in PBS, pH 7.4 ($10^7$ cells/ml), for administration to recipient mice.

### 2.9. Oral OVA challenge model

Recipient female C57BL/6 mice (20–22 g) were administered 50 mg OVA in 0.2 mL of PBS as a single dose, by oral gavage on Day 1. A negative control group received only PBS and was termed the PBS treated group. Each mouse was then administered ~0.2 mL of the cell suspension containing $2 \times 10^6$ donor $CD4^+$ or $CD8^+$ T cells from the OT mice (purified and labelled as per Section 2.8), via the tail vein within 0.5–3 h of OVA administration. The OVA dosed mice were then divided into four treatment groups and administered different treatments via oral gavage. One group received no additional treatment (OVA treated group), a second received 50 mg/kg MPA as a suspension in 0.2 mL of 0.5% CMC (OVA+MPA treated group), and a third received the MPA-TG prodrug at a molar dose equivalent to 50 mg/kg of MPA, formulated in a lipid emulsion (OVA+MPA-TG treated group). A fourth group received

blank lipid emulsion vehicle (OVA+Lipid vehicle treated group).

Two different treatment protocols were followed for the oral OVA challenge studies as described in detail in supplementary Fig. S-1 and summarised in Fig. 5A, 6A and 7A. The first was the 'late treatment protocol' (Fig. 5A). Here the treatments were administered on days 2, 3 and 4, twice a day in the morning and evening (i.e. 6 doses). The second was the 'early treatment protocol' (Fig. 6A), where the treatment was initiated earlier on day 1 after the administration of the T cells. Thereafter the treatments were administered on the following 3 days (total 7 doses), at a regular interval of 10–12 h.

In both the early and late treatment protocols, the mice were killed on day 5 and the MLN (a pooled combination of upper MLN draining the duodenum and lower MLN draining the jejunum and the ileum) and PLN (a pooled combination of inguinal, axillary, brachial, and cervical lymph nodes) were collected and analysed by flow cytometry (as below) to assess the proliferation of OVA specific T cells.

### 2.10. Peripheral OVA challenge model

In the peripheral challenge model, only $CD8^+$ T cells (from OT-I mice) were used because these were the conditions under which the largest PLN effects were seen after oral challenge. $CD8^+$ T cells were harvested from OT-I mice and labelled with CTV as described above. In this model the OVA was administered via subcutaneous (sc) administration into the foot pad rather than via the oral route, to examine whether the oral prodrug was able to inhibit T cell proliferation in PLNs (popliteal, inguinal and iliac). The experimental design is depicted in Fig. S-2 in the supplementary information. OVA in incomplete Freund's adjuvant (IFA) was prepared by first pipetting 300 μL IFA into 1.5 mL Eppendorf tubes. A solution of 6 mg of OVA dissolved in 300 μL PBS, pH 7.4, was then added, drop by drop into the tube containing IFA, with continuous vortexing to form a thick emulsion of OVA in IFA. On day 1, 10 μl of the emulsion of OVA in IFA (10 μg/μl) was administered to each foot pad in the mice, giving a total exposure of 200 μg of OVA per mouse. The purified $CD8^+$ T cells ($2 \times 10^6$) were then injected via the tail vein within 3 h after OVA as described in the oral challenge model. The different treatment groups remained the same as in the oral challenge model. The negative control group received PBS injected SC into the hind leg and was termed the PBS treated group. The OVA treated group received no additional treatment while the OVA+MPA, OVA+MPA-TG and OVA+Lipid vehicle treatment groups received MPA, MPA-TG and blank lipid formulation, by oral gavage on day 1, 30 min after administration of labelled T cells and twice daily for the next 3 days (every 10–12 h), respectively. This was the same as the early treatment protocol used in the oral OVA challenge model. On day 5, the mice were sacrificed (at 10–12 h after the last dose on day 4), and the MLN (both the upper MLN draining the duodenum plus the lower chain of MLN draining the jejunum and the ileum) and PLN (popliteal, inguinal and iliac lymph nodes) were collected to assess the proliferation of OVA specific T cells by flow cytometry.

### 2.11. Quantification of T cell proliferation in LNs by flow cytometry

For flow cytometry analysis, cells were isolated from the MLN and PLN collected from recipient mice and formed into a single cell suspension in PBS buffer containing 2% FBS. The cells were then incubated for 20 min at 4 °C with either FITC anti-mouse CD45.1 antibody or FITC anti-mouse TCR Vα2 antibody and APC anti-mouse $CD8\alpha^+$ antibody (to label $CD8^+$ cells) or PE anti-mouse CD4 antibody (to label $CD4^+$ cells). Cells were then washed with flow buffer (PBS containing 2% FBS). All antibodies were used at dilutions suggested by the manufacturer (Biolegend). Propidium iodide, 10 ng/ml, was added to the cells prior to flow cytometry to stain the dead cells. Cells that were double positive for CD4 or CD8 and CD45.1 or TCR Vα2 (i.e. CD4 or CD8 lymphocytes derived from OT mice) were selected for analysis of CTV fluorescence, using the Pacific blue filter (450/50). One million total events were acquired by the flow cytometer (BD Biosciences FACSCanto II analyser, Becton, Dickinson and Company, NJ, USA) and data was analysed using FlowJo software version 10.6, by Tree Star Inc., Ashland, OR, USA.

### 2.12. Analysis of MPA and MPA-TG in formulations, lymph, plasma and lymph nodes

Formulation, lymph, plasma and LN samples were processed and analysed for free MPA and MPA glyceride derivatives using a validated HPLC-MS/MS as described previously [34] and in the supplementary information section 7.

### 2.13. Statistical analysis

Statistical differences were determined by one-way or two-way ANOVA followed by Dunnett's or Bonferroni's test for multiple comparisons at a significance level of $p = 0.05$. GraphPad Prism for Windows V8.1.2 software (GraphPad Software Inc., CA, USA) was used for analysis. Mean ± SEM was calculated for all parameters except for Tmax for which median and range is reported.

## 3. Results

### 3.1. The lymphatic transport of total MPA is significantly higher in mice after administration of MPA-TG compared to MPA

The total recovery of MPA-related species in the lymph (present as either drug or glyceride derivatives) over time (as a % dose) is shown in Fig. 3A. Lymphatic recovery of MPA derivatives was significantly higher after intraduodenal administration of MPA-TG in the LBF (11.7% dose over 6 h, $p < 0.05$) when compared to MPA in an aqueous solution formulation (0.14% over 6 h). Since the pro/drugs were administered as an intraduodenal infusion for 1 h, a lag in lymphatic transport for MPA-TG was observed during the first hour. Cumulative lymphatic transport increased up to 4 h and then plateaued, suggesting little ongoing transport into lymph after this time. In order to verify whether the higher lymphatic transport of MPA-TG compared to MPA was due to co-administration with the LBF, lymphatic transport of unconjugated MPA was also tested on co-administration with a LBF. Co-administration of lipid had no discernible effect on the lymphatic transport of MPA when compared to the aqueous solution of MPA.

The total mass of MPA derivatives (in μg) that was transported into lymph over 6 h was also calculated (Fig. 3B). The data in Fig. 3B are dose normalised to a nominal dose of 12.5 mg/kg. MPA transport in lymph was 83-fold higher after administration of MPA-TG compared to MPA (aqueous formulation) (29.12 μg vs 0.35 μg) and 153-fold higher than for MPA (LBF) (29.12 μg vs 0.19 μg). Fig. 3C provides a comparison of the concentration of total MPA-related species in lymph after administration of MPA-TG versus MPA showing a similar scale (~2 orders of magnitude) of increase in exposure after administration of the prodrug.

### 3.2. Plasma exposure of MPA is similar in mice after administration of MPA and MPA-TG

The plasma exposure of MPA was determined after administration of an equivalent dose of MPA (50 mg/kg) to the mice in the form of parent drug or MPA-TG prodrug. This dose has been shown previously to inhibit T cell proliferation in mice [43]. The results of the plasma pharmacokinetics study indicate that the exposure of MPA in plasma after administration of both parent drug and prodrug was similar (Fig. 3D). To evaluate the potential for prodrug accumulation during multiple dosing in the OVA challenge studies, a multi-dose pharmacokinetics study was also conducted for MPA and MPA-TG (Fig. 3E). Mice were dosed twice daily for 5 doses and blood/plasma samples were collected over time following the last dose. Slightly higher pre-dose (ie. time 0) plasma concentrations of MPA were observed for MPA-TG

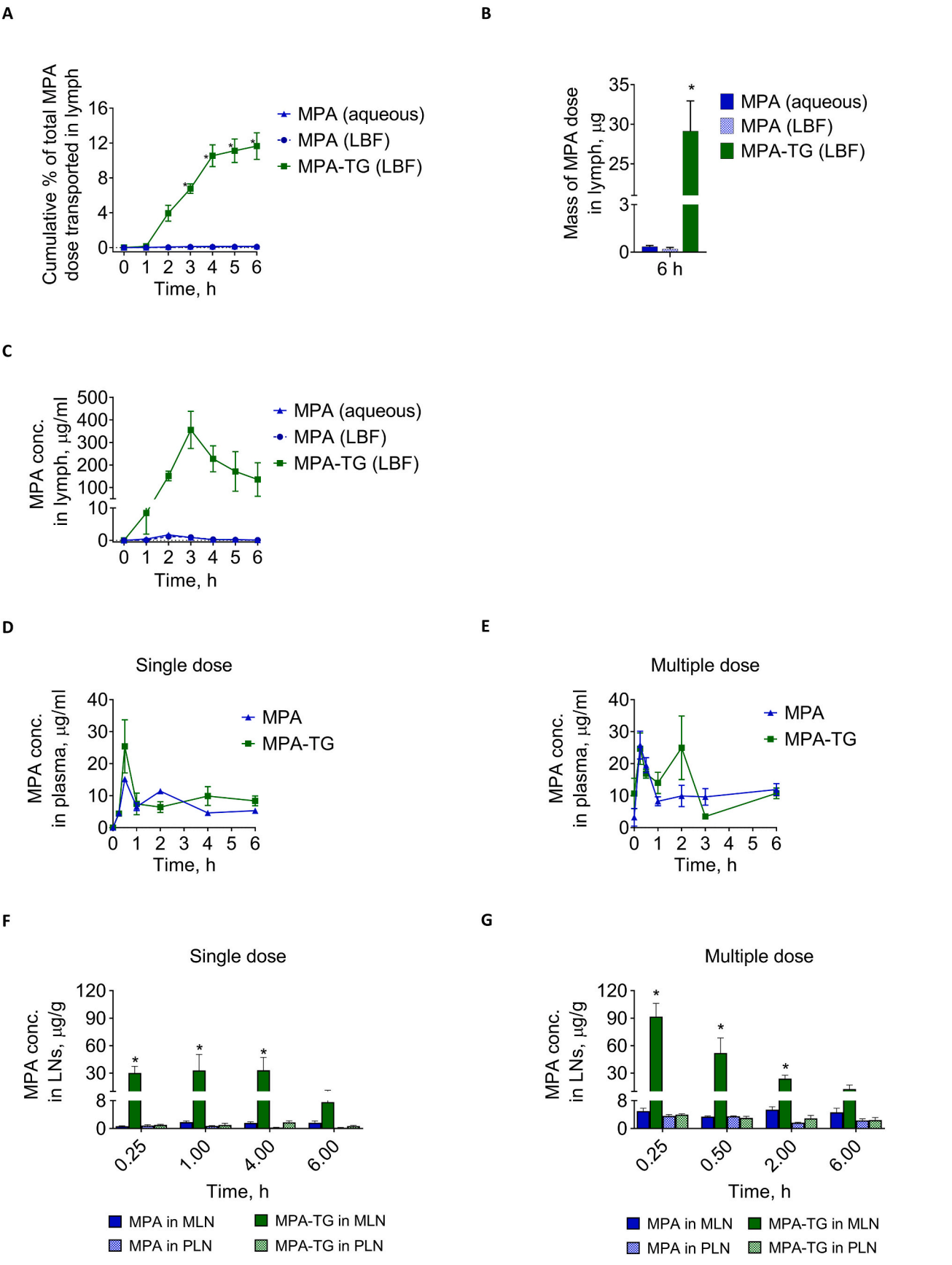


*(caption on next page)*

**Fig. 3.** A) Cumulative lymphatic transport of total MPA-related derivatives (present as MPA and MPA-glycerides) as a % of the dose of MPA (MPA administered as MPA or MPA-TG). B) Mass and C) Concentration of MPA-related derivatives in lymph (expressed as MPA equivalent concentration) over 6 h after dose normalising to a 12.5 mg/kg equivalent dose of parent MPA. Data are presented as mean ± SEM for MPA aqueous ($n$=3) and MPA-TG ($n$=6) and as mean ± range for MPA LBF ($n$ = 2). * indicates significant difference ($p < 0.05$) vs MPA aqueous. D) MPA plasma concentration versus time profiles following oral gavage of a single dose of MPA or MPA-TG prodrug to conscious mice. Data are presented as mean ± SEM, n=3 at each time point. E) MPA plasma concentration versus time profile of MPA following oral gavage of MPA, and MPA-TG prodrug to conscious mice after multiple-dose administration of 5 doses every 10–12 h. Data are presented as mean ± SEM, n=4 at each time point. MPA and MPA-TG were administered at a 50 mg/kg equivalent MPA dose. F) MPA concentration in LNs following oral gavage of a single dose of MPA and MPA-TG prodrug to conscious mice. G) MPA concentration in LNs following oral gavage of MPA and MPA-TG prodrug after multiple-dose administration of 5 doses every 10–12 h. Data are presented as mean ± SEM, n=3 at each time point for single and n= 4 for multiple dose studies. * indicates statistical differences between MPA-TG and other groups ($p < 0.05$).

compared to MPA after multiple dose administration. However, the $C_{max}$ and $AUC_{(0\text{-}6h)}$ values for MPA in plasma did not show any significant differences between the groups administered multiple doses of MPA or MPA-TG. A summary of the pharmacokinetic parameters calculated by non-compartmental analysis is listed in the supplementary information, Table S-2. No statistically significant differences were apparent for plasma pharmacokinetics parameters after either single or multiple-dose administration of MPA and MPA-TG. There was a second peak in plasma concentration at ~2 to 4 h following dosing in both the single- and multiple-dose treatment regimens. This is likely due to the enterohepatic recirculation of MPA, as documented in earlier studies in rats and humans [44,45]. The similar plasma exposure of MPA after dosing MPA-TG and MPA suggests that a significant portion of MPA is ultimately released from the MPA-TG prodrug following entry into the blood circulation.

### 3.3. MPA exposure in the MLN is enhanced after administration of MPA-TG compared to MPA

The concentration of MPA released in the MLN is expected to be the most direct indicator of the potential efficacy of the prodrug in inhibiting T cell replication in the MLN. The concentrations of MPA in the MLN and, as a comparison in PLN, after both single- and multiple-dose administration of MPA and MPA-TG are shown in Fig. 3F, G. On average there was a ~ 20-fold higher concentration of MPA in the MLN after administration of the prodrug when compared to administration of MPA up to 4 h after single-dose administration. By contrast, there was no increase in released MPA concentrations in the PLNs after administration of MPA-TG. On multiple compared to single dosing, there was a larger increase in MPA concentrations in the MLN (50–80 fold) at 15 min following MPA-TG dosing and this remained high at 30 min (a time point added in the multiple dose studies to better evaluate early exposure). This initial increase declined to concentrations similar to those observed after single doses at later time points.

A summary of the AUC of released MPA concentrations observed in the MLN and PLN for up to 6 h after single- and multiple-dose administration of both MPA and MPA-TG is provided in the supplementary information in Table S-3. This provides an indication of exposure in the LNs over time. For both the single and multiple-dose treatments with MPA-TG, released MPA exposure in the MLN was significantly higher than in PLN and also significantly higher than after administration of the parent drug MPA. The cumulative AUC for multiple doses was higher than that determined for a single dose, but this may reflect the fact that earlier time points were sampled in the multiple-dose experiments when compared to the single-dose study.

### 3.4. Administration as a TG mimetic prodrug results in co-localisation of a model fluorescent probe (Bodipy) with immune cells in the MLN

To investigate the potential for the TG mimetic prodrug approach to enhance drug access to immune cell populations in the MLN and PLN, we synthesised a TG mimetic prodrug where MPA was replaced with the fluorescent probe Bodipy (BDP-TG) to allow visualisation of trafficking. The intestinal lymphatic transport of BDP-TG was first examined to confirm integration into the same lymphatic transport pathways as MPA-TG. Lymphatic transport of BDP-TG was studied in rats and ~ 28% of the administered dose was recovered in lymph over a 6 h post dose period (see supplementary Fig. S-8). BDP-TG was thus deemed to be a suitable tool to probe distribution within the intestinal lymphatics, MLN and the immune cells therein, recognising that the tool compound (BDP-TG) is structurally different to MPA-TG and may not behave identically. Disposition of BDP-TG to immune cells within the MLN (at 1, 5 and 10 h) and PLN (at 1 h) was analysed by fluorescence microscopy and flow cytometry. In the imaging experiments, at the early time point (1 h), large quantities of Bodipy was present in the periphery of the node, likely in the sub-capsular sinus (SCS) and medulla and penetration into the B cell and T cell zones appeared to be lower (Fig. 4A and supplementary information, Fig. S-3). In contrast, Bodipy was undetectablein MLN after oral administration of Bodipy alone ie.parent (Supplementary information Fig. S-4). Similarly in the PLN, no traces of Bodipy were seen even after administration of BDP-TG (Supplementary information, Fig. S-4), in agreement with the pharmacokinetic findings that the TG mimetic prodrug approach leads to high concentrations in the MLN but only minimal exposure in the PLN. At later time points (5 and 10 h after dosing Bodipy-TG), Bodipy levels were lower, but appeared to have distributed from the SCS region and was more widespread in both the B and T cell zones within the MLN (Fig. 4A).

To further quantify Bodipy association with different immune cell subtypes, the association of Bodipy with different cell types was analysed by flow cytometry at 1, 5 and 10 h after administration of BDP-TG. The data are presented as both the proportional distribution of Bodipy positive cells (Fig. 4C) and the proportion of each cell type that was Bodipy positive ($BDP^+$) (Fig. 4D). Overall, Bodipy showed broad association with $CD4^+$ T cells (up to 20% of $BDP^+$ cells were $CD4^+$ T cells), $CD8^+$ T cells (up to 10%) and $CD19^+$ B cells (~20%) whereas fewer of the $BDP^+$ cells were $CD11b^+F4/80^+$ macrophages and $CD11c^+$ dendritic cells (<3% of $BDP^+$ cells were macrophages and dendritic cells, presumably reflecting their lower prevalence compared to lymphocytes) (Fig. 4B). Consistent with the imaging data in Fig. 4A, the proportion of $BDP^+$ cells that were $CD4^+$ and $CD8^+$ T cells was significantly lower at 1 h and increased at 5h and to a lesser extent at 10h. In contrast, association with B cells, macrophages and dendritic cells was relatively consistent across all timepoints. Analysis to determine the proportion of each cell type that was $BDP^+$, revealed that at later time points up to 60% of dendritic cells, macrophages and B cells were $BDP^+$, whereas a slightly smaller proportion (up to 50%) of T cells were $BDP^+$. This was even more evident at early time points for $CD8^+$ T cells (and to a lesser extent $CD4^+$) where a smaller proportion of cells were $BDP^+$ (30% for $CD8^+$ and 40% for $CD4^+$). The data suggest that BDP-TG that enters through the SCS is taken up relatively rapidly by macrophages (or dendritic cells) or may enter in association with dendritic cells, and levels in these cells remain high up to 10 h (60% of macrophages and dendritic cells are $BDP^+$). Exposure to B cells is also relatively high even at early time points, consistent with the location of B cells closer to the SCS. In contrast, exposure to T cells in the cortex, further removed from the SCS, is lower especially at earlier time points, but increases over time. Notably, the FACS data does not capture non-cell associated BDP, which the imaging data suggests is high at 1 h.

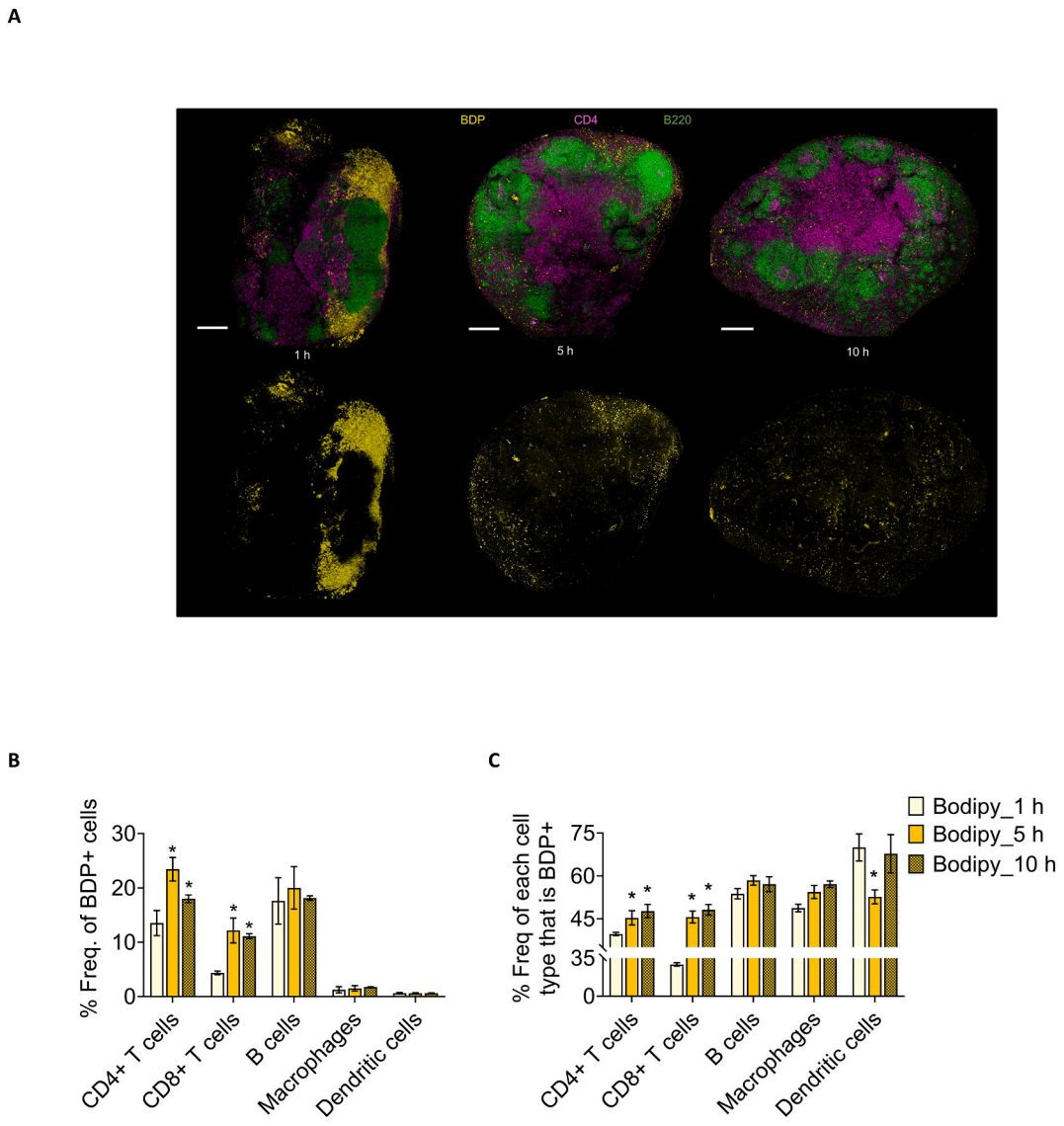


**Fig. 4.** Distribution and immune cell association of Bodipy in MLN after administration of BDP-TG. A) Representative images showing distribution of Bodipy (yellow) within the MLN and co-localisation with $CD4^+$ cells (pink), and $B220^+$ B cells (green). Scale bar shows 200 μm. B) Flow cytometry analysis showing the frequencies of $CD4^+$ and $CD8^+$ T cells, $CD19^+$ B cells, $CD11b^+F4/80^+$ macrophages and $MHCII^+CD11c^+$ dendritic cells within total $BDP^+$ cells in MLN at 1 h, 5 h and 10 h after oral gavage. C) Flow cytometry analysis showing the frequencies of $BDP^+$ $CD4^+$ and $CD8^+$ T cells, $CD19^+$ B cells, $F4/80^+$ macrophages and $CD11c^+$ dendritic cells in MLN at 1 h, 5 h and 10 h after oral gavage. Data are presented as mean ± SD, $n = 3$ at all timepoints. Statistical differences were assessed by one-way ANOVA with Dunnett's multiple comparison to data at the 1 h timepoint. * indicates $p < 0.05$. (For interpretation of the references to colour in this figure legend, the reader is referred to the web version of this article.)

### *3.5. MPA-TG inhibits T cell responses in the MLN more effectively than parent MPA after oral antigen challenge*

To examine the immunosuppressive effect of MPA, the proliferation of adoptively transferred $OVA_{329–337}$ $IA^b$-specific $CD4^+$ OT-II cells was measured in both MLN and PLN in mice challenged with oral OVA and treated with PBS control, MPA or MPA-TG via oral gavage (see Fig. 5A timeline). Proliferation was assessed by flow cytometry measurements of the dilution of CTV staining in the transferred $CD4^+$ OT-II cells (Fig. 5B). In mice challenged with oral OVA the CTV fluorescence intensity was diluted in each generation of cells. In contrast, in the PBS control group that was not administered OVA, ~ 99% of the transferred $CD4^+$ OT cells retained the maximum intensity of the dye during the experiment and remained in the parent (G0) generation. This is indicative of a lack of T cell response in the PBS control group, as expected. In the groups that were administered OVA and not further treated (OVA) or that were administered OVA and treated with MPA (OVA+MPA), MPA-TG (OVA+MPA-TG) or lipid vehicle (OVA+Lipid vehicle) the degree of cell proliferation varied. In the MPA-TG treated group there appeared to be a higher proportion of cells in the lower generations and thus a more profound inhibition of T cell proliferation compared to the control and MPA treated groups. In the OVA and lipid vehicle control groups, T cell proliferation was efficient as expected. In the MPA group some inhibition of T cell proliferation was evident but this was not as potent as the effect of MPA-TG.

To quantify the response of the different treatment groups, Fig. 5C, E shows the cumulative percentage of cells in each generation after administration of the different treatments. In the MLN (Fig. 5C, E), in the absence of OVA stimulation, 100% of cells remained at generation zero (G0). In the OVA alone group and OVA plus Lipid vehicle group, robust cell proliferation was evident and only ~25% of cells remained in G0-G4. In contrast, the MPA-TG treated mice showed significantly inhibited T cell proliferation and ~ 80% of the OT-II cells were retained within G0-G2. For the MPA treated group, there was more limited inhibition of

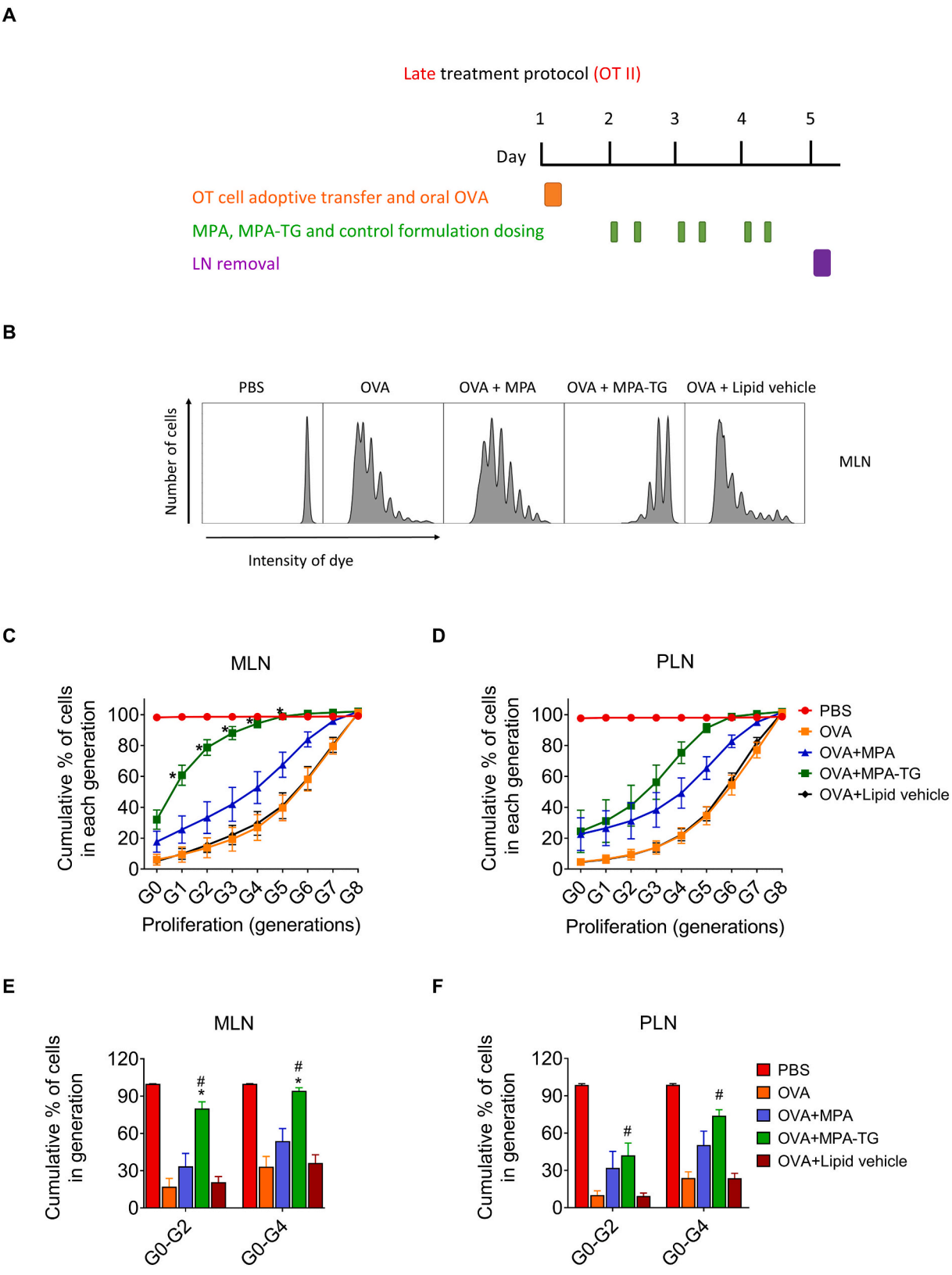


**Fig. 5.** A) The experimental design of the $CD4^+$ T cell response experiments in the oral OVA challenge model. B) Representative flow cytometry histograms showing the proliferation of CTV labelled $CD4^+$ T cells derived from OT-II mice in the MLN of recipient mice. The inhibition of $CD4^+$ T cell proliferation in MLN (C) and PLN (D), after oral administration of PBS, OVA, MPA, MPA-TG and lipid vehicle. E) and F) show the percentage cells within generation 0–2 and generation 0–4 in MLN and PLN respectively for the five treatment groups. Data are representative of two independent experiments with 3–4 mice per group except for the PBS group where $n = 2$ mice were used in each experiment. * indicates $p$ value $<0.05$ vs MPA and # indicates $p$ value $<0.05$ vs OVA (positive control) group.

T cell proliferation and less than 60% of cells were present in G0-G4. In the PLN (Fig. 5D, F), both MPA-TG and MPA showed moderate suppression of T cell proliferation and as expected the degree of suppression of T cell proliferation was similar in both MLN and PLN for MPA (since distribution of MPA is expected to be non-specific). Interestingly, whilst the effect of MPA-TG was greater in the MLN, reflecting mesenteric lymph targeted delivery, there was also a trend toward slightly better suppression of T cell proliferation in the PLN when compared to MPA. MPA-TG thus inhibits $CD4^+$ T cell proliferation in the MLN more effectively than parent MPA after oral antigen challenge.

In studies analogous to those described above for $CD4^+$ T cells, OVA sensitive $CD8^+$T cells from OT-I mice were adoptively transferred into syngeneic C57BL/6 mice and stimulated via oral administration of 50 mg of OVA or PBS. The OVA dosed mice were further treated with either MPA, MPA-TG, LBF control or were left untreated. Both early and late treatment protocols were employed (Fig. 6A and supplementary information Fig. S-1). Consistent with the $CD4^+$ T cell data, $OVA_{257–264}$H-2 K-$^b$-specific $CD8^+$ OT-I T cells actively proliferated in response to OVA, whilst the PBS treated group showed no proliferation. Unlike the $CD4^+$ T cell experiments, however, using the late treatment protocol (ie. when the drug treatments were initiated on day 2), neither MPA nor MPA-TG were able to suppress T cell replication in the MLN or PLN (see supplementary information Fig. S-6). We hypothesised that this could be due to more aggressive and rapid proliferation of $CD8^+$ T cells as compared to $CD4^+$ T cells, since the cell division time for $CD8^+$ T cells is shorter than that for $CD4^+$T cells (8 h vs 11 h) [46]. The decision was

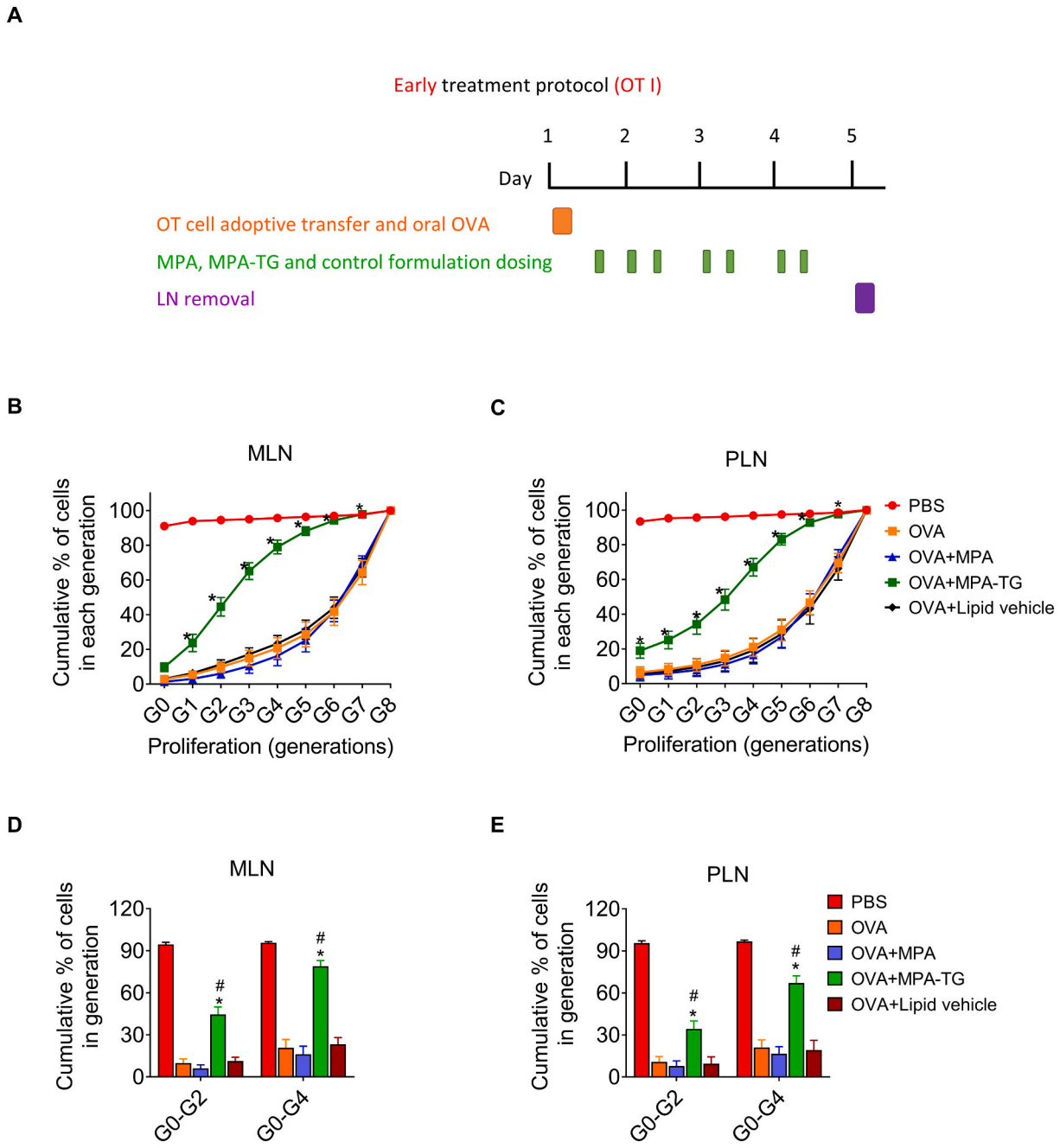


**Fig. 6.** A) The experimental design of the $CD8^+$ T cell response experiments in the oral OVA challenge model. The inhibition of $CD8^+$ T cell proliferation in B) MLN and C) PLN after oral administration of PBS, OVA, MPA, MPA-TG and lipid vehicle. D) and E) show the percentage of cells within generation 0–2 and generation 0–4 in MLN and PLN, respectively. Data are representative of two independent experiments with 3–4 mice per group except for the PBS group where $n = 2$ mice were used in each experiment. * indicates $p$ value $<0.05$ vs MPA and $^{\#}$ indicates $p$ value $<0.05$ vs OVA (positive control) group.

therefore made to initiate treatment earlier, i.e. on day 1 immediately after the administration of OVA (ie. the early treatment protocol - see timeline in Fig. 6A).

Using the early treatment protocol, the inhibitory effect of MPA-TG re-emerged in the MLN (e.g. 80% of $CD8^+$ T cells were present in G0–4) (Fig. 6B, D) and this effect was greater than that of MPA (<30% restricted to G0–4). The lipid vehicle control had no effect on suppression of T cell responses in the MLN. Interestingly, a similar OT-I T cell proliferation profile was observed in the PLN (Fig. 6C, E) and in the Peyer's patches (PP) (Fig. S-7) as was observed in the MLN, across all the treatment groups. Since the beneficial effect of the lymph directed prodrug MPA-TG was not expected in PLN, this was hypothesised to reflect inhibition of T cells in the MLN followed by recirculation of cells from the MLN to the PLN by day 5. This hypothesis stimulated further studies to explore whether similar effects were apparent when an immune response was stimulated in the PLNs via subcutaneous (SC) administration of OVA (see below).

For completeness, experiments were also repeated for OT-II cells using the same early treatment protocol used for OT-I cells. These data are shown in supplementary Fig. S-5 and were essentially the same as that described above for the early treatment protocol, with the exception of a small effect of the vehicle. Unlike OT-I cells, OT-II cells therefore appear to be less sensitive to variations in treatment timing.

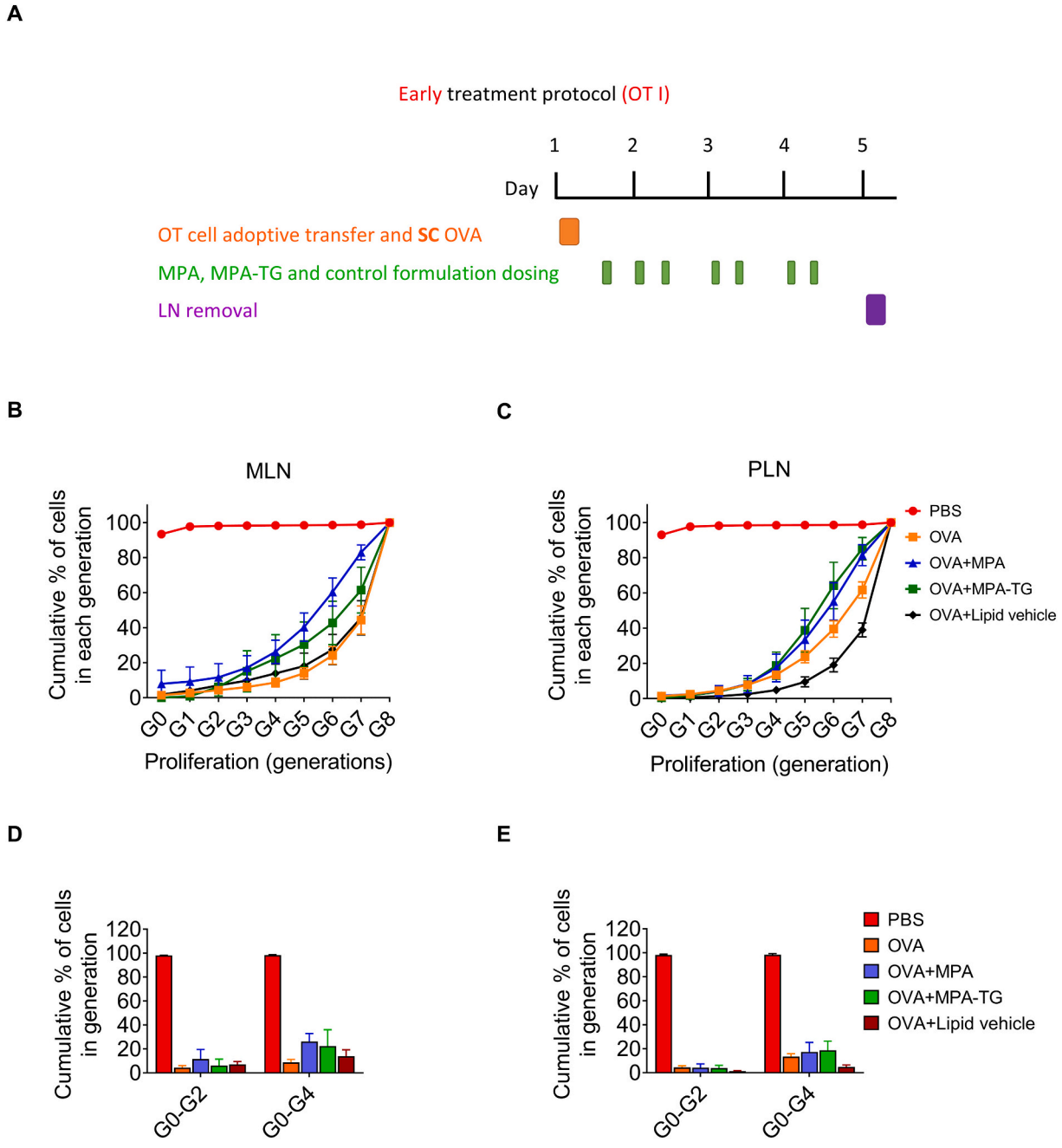


**Fig. 7.** A) The experimental design of the $CD8^+$ T cell response experiments in the peripheral OVA challenge model. Inhibition of $CD8^+$ T cells in B) MLN and C) PLN after administration of PBS, OVA, MPA, MPA-TG and lipid vehicle. D) and E) show the percentage of cells within generation 0–2 and generation 0–4 in MLN and PLN. Data are representative of two independent experiments with 3–4 mice per group except for the PBS group where $n = 2$ mice were used in each experiment. No statistical significant differences were found between the treatment groups and OVA.

### 3.6. Oral MPA-TG specifically inhibits gut-initiated T cell responses

In light of the apparent effects of MPA-TG on T cell proliferation in PLN, experiments were conducted to examine whether MPA-TG is able to inhibit OVA induced T cell proliferation when the immune challenge occurs peripherally rather than via oral administration (where T cell proliferation occurs predominantly in the MLN). To achieve this, a peripheral OVA challenge model was used. In this study, $CD8^+$ T cells from OT-I mice were employed (since this was the group where the largest PLN effect was apparent in previous studies, Fig. 6) and based on the data above, the early treatment protocol was used (see Fig. 7A timeline). In the peripheral challenge model, OVA was administered via SC injection into the hind leg and the T cell response was therefore expected to occur initially in the PLN draining the leg including the popliteal, inguinal and iliac nodes and subsequently throughout the body, including in the MLN.

As expected, SC injection of OVA led to robust stimulation of OT-I T cell proliferation in both the PLN and MLN. In contrast in the PBS control group, OT-I T cells did not proliferate in either the PLN or MLN. Animals receiving an injection of OVA were then treated with oral MPA, MPA-TG or vehicle control. MPA and MPA-TG showed limited effects on T cell responses in both the MLN and PLN and no advantage was observed for MPA-TG when compared to MPA in either MLN or PLN as shown in Fig. 7. The small and similar effect for MPA-TG and MPA in both MLN and PLN most likely reflects effects mediated by drug exposure in plasma which was similar for both MPA and MPA-TG. The data thus suggest that the ability of the prodrug to more effectively inhibit T cell proliferation in the PLN when compared to MPA after oral administration of OVA (Fig. 6B) is a function of high concentrations of MPA in the MLN after administration of prodrug and that any spill over effects in PLN were due to migration of T cells that were 'treated' initially in the MLN.

## 4. Discussion

Directed drug delivery to LNs has the potential to show benefit in the treatment of pathologies such as organ transplantation rejection, autoimmune disease, HIV and cancer, in which cells within LNs play a role in disease progression [13–16,19]. We have previously demonstrated in rats and dogs that targeted drug delivery to the MLN can be achieved by piggybacking drug absorption onto endogenous dietary lipid transport pathways that drain into mesenteric lymph using a prodrug approach that mimics the structure of dietary TG [34,35]. Here, we first sought to confirm that the TG mimetic prodrug approach can also enhance delivery to the mesenteric lymph and the MLN in mice before embarking on immune challenge studies in the mice to provide *in vivo* proof of concept that targeting the MLN using the prodrug approach is able to augment immunomodulation.

The transport of MPA-related species in mesenteric lymph after administration of MPA-TG in mice was 83-fold greater than that after administration of MPA (11.65% vs 0.14%). This is consistent with data reported previously in rats, which showed a 78-fold greater transport of MPA-related materials after administration of prodrug compared to parent MPA (13.4% vs 0.17%) [34]. In greyhound dogs, the lymph transport of prodrug followed a similar trend but was even higher resulting in 280-fold higher transport of MPA-related species after administration of MPA-TG than MPA (36.4% vs 0.13%) [35]. The differences across species could be due to a variety of factors, including differences in the re-esterification of MPA-MG to TG derivatives, the association of the re-synthesised derivatives with LP, the relative doses of co-administered lipids, the storage/mobilisation of LP in enterocytes, enterocyte-based first-pass metabolism or blood versus lymph flow [35,47]. The data are also consistent with previous studies of other lipophilic prodrugs [48,49] and a recent study that described a lipophilic prodrug approach for the delivery of bexarotene and retinoic acid to the intestinal lymphatics in rats [33]. In a related approach Kim et al. recently described a bile acid conjugated nanoparticle that significantly enhanced oral bioavailability of the nanoparticle and was proposed to act by integration into bile acid and lipid processing pathways in the enterocyte [50].

In the current study in mice, the plasma exposure for MPA was similar after administration of prodrug or parent drug. This suggests good conversion of prodrug to drug, at least in plasma. In contrast, in rats, the oral exposure of MPA after dosing prodrug was lower than that of parent drug by a factor of ~2, whereas the AUC for total MPA derivatives after prodrug administration was similar to that of the parent drug [51]. In rats, therefore, conversion of the re-esterified MPA-glyceride species to MPA appeared to be incomplete. In dogs, MPA exposure was similar or slightly higher after administration of prodrug when compared to drug, again suggesting efficient conversion [35]. Efficient conversion of re-esterified MPA-glyceride to MPA in mice may reflect the relatively high levels of lipases reported in mouse plasma when compared to rats [52]. A second peak in the plasma pharmacokinetics of MPA was seen in the current studies in mice at ~2–4 h post-dose. This may be attributed to enterohepatic recirculation of MPA, which has been previously reported [44,45]. Multiple dosing did not significantly affect plasma exposure of MPA after administration of drug or prodrug, suggesting both efficient conversion to MPA and relatively rapid subsequent clearance of MPA.

The recovery of high concentrations of released MPA in the MLN after administration of MPA-TG provides evidence to suggest that the TG-mimetic prodrug approach can efficiently deliver drugs to the MLN. In this case, exposure of released MPA in the MLN was ~20 fold higher after administration of MPA-TG when compared to an equimolar dose of MPA. The data are indicative of good MPA release from the prodrug in the MLN. The concentration of MPA in the MLN after dosing prodrug was also significantly higher than in the PLN. In the PLN, the concentration of MPA was similar after administration of either prodrug or MPA. This is consistent with the hypothesis that the prodrug results in the targeted delivery of high quantities of MPA (presumably in the form of re-esterified MPA-TG) directly into the mesenteric lymph and the MLN, leading to the release of MPA therein, and is not due to entry of systemically circulating chylomicrons (containing MPA-TG) into the MLN (which would be apparent at similar levels in PLN).

To further probe the distribution of the prodrug in the MLN, a fluorescent prodrug was synthesised using Bodipy as a fluorescent model drug. This prodrug was then orally administered to mice in an analogous fashion to the studies with MPA-TG. Immunofluorescent imaging revealed the presence of Bodipy largely in the periphery of the node at 1 h and to a lesser extent in the B cell and T cell zones. Bodipy localisation in the subcapsular sinus (SCS) and medulla and co-localisation with lymphatic endothelial cells (LEC), subcapsular macrophages (SCM) and medullary macrophages (MM) was apparent at this timepoint (see supplementary Fig. S-3). In contrast, at later time points (5 h and 10 h) the label had transferred from the SCS into the node parenchyma and was more distributed into the B cell and T cell zones. It has been reported that SCM are responsible for capturing particulate antigens, immune complexes and lymph-borne viruses, and transferring them to the B cells in the follicles, however the transfer of lipid rich chylomicrons (CM), either intact, or as the lipids contained therein, from SCM to B cells or T cells has not to our knowledge been reported previously [53–55]. To probe cellular distribution further, flow cytometry was employed to quantify association of Bodipy with differing cells types in the MLN. These studies showed higher association of Bodipy with macrophages, dendritic cells and B cells at early time points, and slightly lower association with T cells. At later time points however, association with T cells increased providing good evidence of broad exposure of most LN cells types to Bodipy over a 5–10 h post dose period. The fluorescence data is unable to differentiate between Bodipy-TG and released Bodipy, however the pharmacokinetic data shows good release of free MPA in the MLN, suggesting that the images observed at later time points may, at least in part, reflect released Bodipy rather than intact BDP-TG. Interestingly, a recent study has also shown that intact particulates,

even smaller than CM, are unable to penetrate into the cortex and paracortex of the node via the node conduits, but that this could be facilitated by drug release from the nanoparticle within the node [56]. These findings suggest that BDP-TG (or Bodipy) is likely to be released from CM before entering the node cortex and paracortex at later time points.

In light of the significantly enhanced delivery of MPA to the MLN after oral administration of the MPA-TG prodrug, when compared to MPA alone, subsequent studies sought to examine whether targeted MLN delivery was able to enhance the effect of MPA on T cell responses *in vivo* in the MLN. This was achieved using a mouse model where immune activation in the MLN was achieved by oral administration of the model antigen OVA (44). To allow quantification, fluorescently labelled T cells were adoptively transferred from OT-I or OT-II T cell receptor transgenic mice. The adoptively transferred T cells express T cell receptors specific for OVA presented either by MHC class I in the presence of CD8 (obtained from OT-I transgenic mice) or OVA presented by MHC class II in the presence of CD4 (from OT-II transgenic mice). These OVA specific T cells populate the MLN in recipient mice and are activated upon OVA encounter (in association with MHC class I or class II) and begin to proliferate. Using adoptive transfer of labelled OT cells, the extent of T cell proliferation can be monitored and this in turn allows examination of the relative ability of the lymph directed MPA prodrug (MPA-TG) to suppress T cell proliferation when compared to MPA alone. Antigen-specific T cell proliferation is a key response to antigen recognition by the adaptive immune system [57]. Antigen recognition initiates a cascade of events triggering the transcriptional activation of cytokines, growth factors and cell cycle regulators in activated T cells that allows the proliferation of activated T cells [58]. Studies were conducted using OVA-specific $CD4^+$ T cells (from OT-II mice) and $CD8^+$ T cells (from OT-I mice). This allowed separate experiments to quantify the potential to suppress either $CD4^+$ and/or $CD8^+$ T cell proliferation. Notably, whilst exogenous antigen is typically only weakly presented by MHC class I to $CD8^+$ T cells, the oral OVA challenge has been shown to be cross-presented resulting in $CD8^+$ T cell activation [59].

The data demonstrate significantly enhanced inhibition of T cell proliferation when the same molar quantity of MPA was orally administered as the MPA-TG prodrug when compared to drug (MPA) alone. This effect was equally apparent in studies monitoring $CD4^+$ T and $CD8^+$ T cell proliferation. Interestingly, in studies with $CD8^+$ T cells, a marked advantage was apparent in the efficacy of the prodrug in inhibiting proliferation when an early treatment protocol (and not a late treatment protocol) was used. This was not observed in the case of $CD4^+$ T cells, where a similar suppression profile was apparent regardless of the dosing strategy. This may reflect differences in the dynamics of activation of $CD4^+$ and $CD8^+$ T cells after antigen encounter. Consistent with this suggestion, after infection with lymphocytic choriomeningitis virus (LCMV) the doubling time required for $CD4^+$ T cells after antigen exposure is longer (~ 11 h) than that of $CD8^+$ T cells (~ 8 h) [46]. Slower rates of proliferation of $CD4^+$ T cells have also been reported after stimulation by OVA expressing *Listeria monocytogenes* (LM) and after parenteral immunization of OVA peptide as well as after *in vitro* stimulation with OVA peptide ($OVA_{323–339}$) or anti-CD3 [60–63]. In studies with OVA expressing LM, < 7% of $CD4^+$ T cells that were stimulated to divide, differentiated into interferon ɣ (IFN ɣ) producing effector cells. In contrast, for stimulated $CD8^+$ T cells, differentiation was >85% [63]. These reports led us to hypothesise that inhibiting the more rapid and more effective $CD8^+$ T cell response may require earlier initiation of treatment. The lack of immunosuppression after MPA-TG and MPA administration via the late treatment protocol (where dosing was initiated 1 d after antigen) and markedly enhanced immunosuppression when dosing was initiated immediately after antigen presentation (early treatment protocol) is consistent with this suggestion. It is also consistent with previous studies with MPA where oral administration of 50–100 mg/kg/day, was able to inhibit *in vivo* generation of effector cytotoxic T cells, but *in vitro* incubation of MPA with effector T cells that had been previously activated and stimulated *in vivo*, did not lead to immunosuppression [43]. The lack of effect of MPA on previously activated cytotoxic cells has also been reported using a T cell leukaemia line (Jurkat cells) [64]. Interestingly, beneficial immunomodulation effects of MPA-TG versus MPA were seen in both MLN and PLN. We also found inhibition of ova induced T cell proliferation in the PP, using the early treatment procol with $CD8^+$ T cells derived from OT-I mice (see Fig. S-7). The effect in the PP could be due to direct inhibition of T cell proliferation via uptake or trafficking of the prodrug to the PP, or due to the recirculation/homing of 'treated' MLN derived OT cells to the PP (as described below for effects in the PLN) or a combination of both.

Realising that the lymph directed prodrug was expected to promote drug exposure in the MLN, but not the PLN, the initial data was surprising in that oral administration of MPA-TG was able to better inhibit T cell proliferation in both PLN and MLN when compared to MPA (Fig. 5B, C). Two explanations for this behaviour are apparent. Firstly, that T cells are initially activated by OVA in the MLN and then migrate to PLN where proliferation continues, but that MPA exposure to T cells and subsequent inhibition of T cell proliferation can occur within the MLN prior to cell migration. In this way, events in the PLN essentially mirror events in the MLN. The alternate possibility is that oral OVA is absorbed, traffics to the PLN and stimulates PLN T cell expansion, and that oral MPA-TG preferentially inhibits T cell expansion in the PLN via an unknown mechanism. In support of this hypothesis (i.e. that OVA is absorbed and distributed systemically, leading to T cell activation in the PLN), previous studies have shown evidence of simultaneous proliferation of T cells in both the PLN and MLN within 24 h of oral administration of antigen [65] and evidence of systemic absorption of OVA into both portal and peripheral blood [66]. Interestingly, higher concentrations of OVA have also been reported in the celiac LNs that drain the liver when compared the gut draining MLN [67].

To probe whether orally administered MPA-TG is able to directly inhibit T cell proliferation in the periphery (ie. PLN) rather than in the gut (ie. MLN), studies were therefore conducted where the OVA challenge was initiated via the periphery (SC injection). In these studies, injection of OVA into the hind leg resulted in a robust activation of T cell proliferation in the PLN draining the injection site (popliteal, inguinal and ileac) and also in the MLN. Whether the latter reflects direct activation in the MLN or migration of activated T cells to the MLN from the PLN after OVA activation is unknown. However, in all studies where the immune response was activated via SC administration of OVA, MPA-TG was active, but was unable to provide a treatment benefit when compared to MPA alone.

The MPA-TG prodrug therefore appears to preferentially inhibit T cell proliferation in the gut associated lymphoid tissue, although inhibitory events may be evident elsewhere via T cell migration from the point of activation and inhibition in the MLN (and realising that the MLN contain a large T cell reservoir). This argument is strongly supported by previous studies using a similar model that showed inhibition of peripheral lymphocyte proliferation in response to oral OVA after systemic administration of FTY720, a drug that specifically inhibits the movement of lymphocytes out of the LN. For FTY720, inhibition of lymphocyte recirculation from the MLN to PLN prevented any observable effects in the PLN [25].

## 5. Conclusion

The MLN are a major target for the delivery of immunomodulatory agents that seek to inhibit or stimulate gut-related immune events. Using an oral OVA challenge model we have shown here that a TG mimetic prodrug strategy is able to suppress the proliferation of $CD4^+$ T cells and $CD8^+$ T cells in the MLN significantly more effectively after oral administration when compared to drug alone. In contrast, when the immune response is initiated peripherally, but the prodrug is given orally, preferential immunomodulation is not evident. This suggests that the effects of the prodrug are targeted to the gut and may provide

potential for gut-specific immunomodulation with the attendant benefits of reduced systemic effects. The prodrug approach might therefore be beneficial in conditions which are initiated via immune responses in the MLN such as IBD, food allergy, GIT cancer metastasis and GIT infection.

## Acknowledgements

We are grateful to; to Dr. Yanwei Wu and Prof Jianping Zuo at Shanghai Institute of Materia Medica, Chinese Academy of Sciences for their contributions to preliminary screening and discussion that informed model selection in the current studies and to Ms. Sandy Fung and Mr. Timothy Brown and the Imaging, FACS and Analysis Core, Monash Institute of Pharmaceutical Sciences for assistance with flow cytometry and imaging. We also acknowledge assistance from the Harvard Medical School Centre for Immune Imaging and the HMSTrust analytical laboratory at Monash University. Funding support was received from the Australian Research Council (CE140100036)

## Appendix A. Supplementary data

Supplementary data to this article can be found online at https://doi.org/10.1016/j.jconrel.2021.02.008.

## References

[1] G. Oliver, J. Kipnis, G.J. Randolph, et al., The lymphatic vasculature in the 21st century: novel functional roles in homeostasis and disease, Cell 182 (2) (2020) 270–296.
[2] T.V. Petrova, G.Y. Koh, Biological functions of lymphatic vessels, Science 369 (2020) 6500.
[3] K. Maisel, M.S. Sasso, L. Potin, et al., Exploiting lymphatic vessels for immunomodulation: rationale, opportunities, and challenges, Adv. Drug Deliv. Rev. 114 (2017) 43–59.
[4] T.P. Padera, E. Meijer, L. Munn, The lymphatic system in disease processes and Cancer progression, Annu. Rev. Biomed. Eng. 18 (1) (2016) 125–158.
[5] T.V. Petrova, G.Y. Koh, Organ-specific lymphatic vasculature: from development to pathophysiology, J. Exp. Med. 215 (1) (2018) 35–49.
[6] G.J. Randolph, S. Ivanov, B.H. Zinselmeyer, et al., The lymphatic system: integral roles in immunity, Annu. Rev. Immunol. 35 (2017) 31–52.
[7] N.L. Trevaskis, L.M. Kaminskas, C.J. Porter, From sewer to saviour - targeting the lymphatic system to promote drug exposure and activity, Nat. Rev. Drug Discov. 14 (11) (2015) 781–803.
[8] M. Buettner, U. Bode, Lymph node dissection–understanding the immunological function of lymph nodes, Clin. Exp. Immunol. 169 (3) (2012) 205–212.
[9] R. Roozendaal, R.E. Mebius, G. Kraal, The conduit system of the lymph node, Int. Immunol. 20 (12) (2008) 1483–1487.
[10] M. Bajenoff, J.G. Egen, H. Qi, et al., Highways, byways and breadcrumbs: directing lymphocyte traffic in the lymph node, Trends Immunol. 28 (8) (2007) 346–352.
[11] J.P. Girard, C. Moussion, R. Forster, HEVs, lymphatics and homeostatic immune cell trafficking in lymph nodes, Nat. Rev. Immunol. 12 (11) (2012) 762–773.
[12] J.E. Gretz, A.O. Anderson, S. Shaw, Cords, channels, corridors and conduits: critical architectural elements facilitating cell interactions in the lymph node cortex, Immunol. Rev. 156 (1997) 11–24.
[13] J. Azzi, Q. Yin, M. Uehara, et al., Targeted delivery of immunomodulators to lymph nodes, Cell Rep. 15 (6) (2016) 1202–1213.
[14] B. Bahmani, M. Uehara, L. Jiang, et al., Targeted delivery of immune therapeutics to lymph nodes prolongs cardiac allograft survival, J. Clin. Invest. 128 (11) (2018) 4770–4786.
[15] A. Yeste, M. Nadeau, E.J. Burns, et al., Nanoparticle-mediated codelivery of myelin antigen and a tolerogenic small molecule suppresses experimental autoimmune encephalomyelitis, Proc. Natl. Acad. Sci. U. S. A. 109 (28) (2012) 11270–11275.
[16] Z. Hunter, D.P. McCarthy, W.T. Yap, et al., A biodegradable nanoparticle platform for the induction of antigen-specific immune tolerance for treatment of autoimmune disease, ACS Nano 8 (3) (2014) 2148–2160.
[17] G.M. Ryan, L.M. Kaminskas, C.J. Porter, Nano-chemotherapeutics: maximising lymphatic drug exposure to improve the treatment of lymph-metastatic cancers, J. Control. Release 193 (2014) 241–256.
[18] L. Jeanbart, M.A. Swartz, Engineering opportunities in cancer immunotherapy, Proc. Natl. Acad. Sci. U. S. A. 112 (47) (2015) 14467–14472.
[19] C.V. Fletcher, K. Staskus, S.W. Wietgrefe, et al., Persistent HIV-1 replication is associated with lower antiretroviral drug concentrations in lymphatic tissues, Proc. Natl. Acad. Sci. U. S. A. 111 (6) (2014) 2307–2312.
[20] S.T. Reddy, A.J. van der Vlies, E. Simeoni, et al., Exploiting lymphatic transport and complement activation in nanoparticle vaccines, Nat. Biotechnol. 25 (10) (2007) 1159–1164.
[21] C.M. Jewell, S.C. Bustamante López, D.J. Irvine, In situ engineering of the lymph node microenvironment via intranodal injection of adjuvant-releasing polymer particles, Proc. Natl. Acad. Sci. 108 (38) (2011) 15745.
[22] J.S. Alexander, V.C. Ganta, P.A. Jordan, et al., Gastrointestinal lymphatics in health and disease, Pathophysiology 17 (4) (2010) 315–335.
[23] N.L. Trevaskis, W.N. Charman, C.J. Porter, Lipid-based delivery systems and intestinal lymphatic drug transport: a mechanistic update, Adv. Drug Deliv. Rev. 60 (6) (2008) 702–716.
[24] Avi N. Kogan, U.H. von Andrian, Lymphocyte trafficking comprehensive physiology, in: Handbook of Physiology, The Cardiovascular System, Microcirculation, 2008, pp. 449–482.
[25] T. Worbs, U. Bode, S. Yan, et al., Oral tolerance originates in the intestinal immune system and relies on antigen carriage by dendritic cells, J. Exp. Med. 203 (3) (2006) 519–527.
[26] H.L. Weiner, Oral tolerance for the treatment of autoimmune diseases, Annu. Rev. Med. 48 (1997) 341–351.
[27] L.A. Wolfraim, Treating autoimmune diseases through restoration of antigen-specific immune tolerance, Arch. Immunol. Ther. Exp. 54 (1) (2006) 1–13.
[28] S.D. Miller, D.M. Turley, J.R. Podojil, Antigen-specific tolerance strategies for the prevention and treatment of autoimmune disease, Nat. Rev. Immunol. 7 (9) (2007) 665–677.
[29] D.L. Hirsch, P. Ponda, Antigen-based immunotherapy for autoimmune disease: current status, Immunotargets Ther. 4 (2015) 1–11.
[30] A. Habtezion, L.P. Nguyen, H. Hadeiba, et al., Leukocyte trafficking to the small intestine and colon, Gastroenterology 150 (2) (2016) 340–354.
[31] N.L. Trevaskis, W.N. Charman, C.J. Porter, Targeted drug delivery to lymphocytes: a route to site-specific immunomodulation? Mol. Pharm. 7 (6) (2010) 2297–2309.
[32] A. Zgair, J.B. Lee, J.C.M. Wong, et al., Oral administration of cannabis with lipids leads to high levels of cannabinoids in the intestinal lymphatic system and prominent immunomodulation, Sci. Rep. 7 (1) (2017) 14542.
[33] J.B. Lee, A. Zgair, J. Malec, et al., Lipophilic activated ester prodrug approach for drug delivery to the intestinal lymphatic system, J. Control. Release 286 (2018) 10–19.
[34] S. Han, T. Quach, L. Hu, et al., Targeted delivery of a model immunomodulator to the lymphatic system: comparison of alkyl ester versus triglyceride mimetic lipid prodrug strategies, J. Control. Release 177 (2014) 1–10.
[35] S. Han, L. Hu, Gracia, et al., Lymphatic transport and lymphocyte targeting of a triglyceride mimetic prodrug is enhanced in a large animal model: studies in greyhound dogs, Mol. Pharm. 13 (10) (2016) 3351–3361.
[36] J.D. Mintern, S. Bedoui, G.M. Davey, et al., Transience of MHC class I-restricted antigen presentation after influenza a virus infection, Proc. Natl. Acad. Sci. U. S. A. 106 (16) (2009) 6724–6729.
[37] S.R. Clarke, M. Barnden, C. Kurts, et al., Characterization of the ovalbumin-specific TCR transgenic line OT-I: MHC elements for positive and negative selection, Immunol. Cell Biol. 78 (2) (2000) 110–117.
[38] S.L. Klein, K.L. Flanagan, Sex differences in immune responses, Nat. Rev. Immunol. 16 (10) (2016) 626–638.
[39] M.R. Gubbels Bupp, T.N. Jorgensen, Androgen-induced immunosuppression, Front. Immunol. 9 (794) (2018).
[40] N.L. Trevaskis, S.M. Caliph, G. Nguyen, et al., A mouse model to evaluate the impact of species, sex, and lipid load on lymphatic drug transport, Pharm. Res. 30 (12) (2013) 3254–3270.
[41] B.J. Quah, C.R. Parish, The use of carboxyfluorescein diacetate succinimidyl ester (CFSE) to monitor lymphocyte proliferation, J. Vis. Exp. 44 (2010) 2259.
[42] B.J.C. Quah, A.B. Lyons, C.R. Parish, The use of CFSE-like dyes for measuring lymphocyte proliferation: experimental considerations and biological variables, Math. Model. Nat. Phenom. 7 (5) (2012) 53–64.
[43] E.M. Eugui, A. Mirkovich, A.C. Allison, Lymphocyte-selective antiproliferative and immunosuppressive effects of mycophenolic acid in mice, Scand. J. Immunol. 33 (2) (1991) 175–183.
[44] T. van Gelder, J. Klupp, M.J. Barten, et al., Comparison of the effects of tacrolimus and cyclosporine on the pharmacokinetics of mycophenolic acid, Ther. Drug Monit. 23 (2) (2001) 119–128.
[45] R. Bullingham, S. Monroe, A. Nicholls, et al., Pharmacokinetics and bioavailability of mycophenolate mofetil in healthy subjects after single-dose oral and intravenous administration, J. Clin. Pharmacol. 36 (4) (1996) 315–324.
[46] R.J. De Boer, D. Homann, A.S. Perelson, Different dynamics of CD4+ and CD8+ T cell responses during and after acute lymphocytic choriomeningitis virus infection, J. Immunol. 171 (8) (2003) 3928–3935.
[47] N.L. Trevaskis, G. Lee, A. Escott, et al., Intestinal lymph flow, and lipid and drug transport scale Allometrically from pre-clinical species to humans, Front. Physiol. 11 (2020) 458.
[48] V.J. Stella, SpringerLink, Prodrugs: Challenges and Rewards, Springer: AAPS Press, New York, NY, 2007.
[49] D.M. Lambert, Rationale and applications of lipids as prodrug carriers, Eur. J. Pharm. Sci. 11 (Suppl. 2) (2000) S15–S27.
[50] K.S. Kim, K. Suzuki, H. Cho, et al., Oral nanoparticles exhibit specific high-efficiency intestinal uptake and lymphatic transport, ACS Nano 12 (9) (2018) 8893–8900.
[51] S. Han, L. Hu, T. Quach, et al., Profiling the role of deacylation-reacylation in the lymphatic transport of a triglyceride-mimetic prodrug, Pharm. Res. 32 (5) (2015) 1830–1844.
[52] J. Peterson, G. Bengtsson-Olivecrona, T. Olivecrona, Mouse preheparin plasma contains high levels of hepatic lipase with low affinity for heparin, Biochim. Biophys. Acta 878 (1) (1986) 65–70.

[53] Y.R. Carrasco, F.D. Batista, B cells acquire particulate antigen in a macrophage-rich area at the boundary between the follicle and the subcapsular sinus of the lymph node, Immunity 27 (1) (2007) 160–171.
[54] T.G. Phan, I. Grigorova, T. Okada, et al., Subcapsular encounter and complement-dependent transport of immune complexes by lymph node B cells, Nat. Immunol. 8 (9) (2007) 992–1000.
[55] T. Junt, E.A. Moseman, M. Iannacone, et al., Subcapsular sinus macrophages in lymph nodes clear lymph-borne viruses and present them to antiviral B cells, Nature 450 (7166) (2007) 110–114.
[56] A. Schudel, A.P. Chapman, M.-K. Yau, et al., Programmable multistage drug delivery to lymph nodes, Nat. Nanotechnol. 15 (6) (2020) 491–499.
[57] A. Mayer, Y. Zhang, A.S. Perelson, et al., Regulation of T cell expansion by antigen presentation dynamics, Proc. Natl. Acad. Sci. 116 (13) (2019) 5914–5919.
[58] J.E. Smith-Garvin, G.A. Koretzky, M.S. Jordan, T cell activation, Annu. Rev. Immunol. 27 (2009) 591–619.
[59] E. Blanas, G.M. Davey, F.R. Carbone, et al., A bone marrow-derived APC in the gut-associated lymphoid tissue captures oral antigens and presents them to both CD4+ and CD8+ T cells, J. Immunol. 164 (6) (2000) 2890–2896.
[60] R. Merica, A. Khoruts, K.A. Pape, et al., Antigen-experienced CD4 T cells display a reduced capacity for clonal expansion in vivo that is imposed by factors present in the immune host, J. Immunol. 164 (9) (2000) 4551–4557.
[61] H. Gudmundsdottir, A.D. Wells, L.A. Turka, Dynamics and requirements of T cell clonal expansion in vivo at the single-cell level: effector function is linked to proliferative capacity, J. Immunol. 162 (9) (1999) 5212–5223.
[62] A.M. Doyle, A.C. Mullen, A.V. Villarino, et al., Induction of cytotoxic T lymphocyte antigen 4 (CTLA-4) restricts clonal expansion of helper T cells, J. Exp. Med. 194 (7) (2001) 893–902.
[63] K.E. Foulds, L.A. Zenewicz, D.J. Shedlock, et al., Cutting edge: CD4 and CD8 T cells are intrinsically different in their proliferative responses, J. Immunol. 168 (4) (2002) 1528–1532.
[64] G. Strauss, W. Osen, K.M. Debatin, Induction of apoptosis and modulation of activation and effector function in T cells by immunosuppressive drugs, Clin. Exp. Immunol. 128 (2) (2002) 255–266.
[65] K.M. Smith, J.M. Davidson, P. Garside, T-cell activation occurs simultaneously in local and peripheral lymphoid tissue following oral administration of a range of doses of immunogenic or tolerogenic antigen although tolerized T cells display a defect in cell division, Immunology 106 (2) (2002) 144–158.
[66] T. Matsubara, N. Aoki, T. Honjoh, et al., Absorption, migration and kinetics in peripheral blood of orally administered ovalbumin in a mouse model, Biosci. Biotechnol. Biochem. 72 (10) (2008) 2555–2565.
[67] F.M. Oliveira, E.M. Dos Santos, A.C. Alves, et al., Digestion, absorption and tissue distribution of ovalbumin and palmitoyl-ovalbumin: impact on immune responses triggered by orally administered antigens, Scand. J. Immunol. 65 (2) (2007) 139–147.